Western Graduate&PostdoctoralStudies

Western University
Scholarship@Western

Electronic Thesis and Dissertation Repository

1-6-2021 4:00 PM

Exploring Methods for Improving Baseplate Fixation in Reverse Total Shoulder Arthroplasty

Sejla Abdic, *The University of Western Ontario*

Supervisor: Johnson, James A., *Roth McFarlane Hand and Upper Limb Clinic*
Joint Supervisor: Athwal, George S., *Roth McFarlane Hand and Upper Limb Clinic*
A thesis submitted in partial fulfillment of the requirements for the Master of Science degree in Surgery
© Sejla Abdic 2021

Follow this and additional works at: https://ir.lib.uwo.ca/etd

 Part of the Orthopedics Commons

Recommended Citation

Abdic, Sejla, "Exploring Methods for Improving Baseplate Fixation in Reverse Total Shoulder Arthroplasty" (2021). *Electronic Thesis and Dissertation Repository*. 7624.
https://ir.lib.uwo.ca/etd/7624

This Dissertation/Thesis is brought to you for free and open access by Scholarship@Western. It has been accepted for inclusion in Electronic Thesis and Dissertation Repository by an authorized administrator of Scholarship@Western. For more information, please contact wlswadmin@uwo.ca.

Abstract

Improving the success of modern reverse shoulder replacements is dependent on optimal baseplate fixation. A cadaveric biomechanical investigation examined how peripheral screw position and orientation affect baseplate fixation in normal glenoids. The results show no statistically significant difference between screw position (p=.60) or orientation (p=.20) regarding baseplate micromotion in the non-eroded glenoid. In a subsequent study to determine best management in pathologic baseplate fixation, a computer-model was employed to quantify the erosion in the E2 type glenoid. In the E2 type glenoid, erosion was found to be oriented postero-superiorly and covering an average of 66% of the surface area of the glenoid, requiring a full augmented baseplate for best seating. Overall, these findings support aiming peripheral screws into best quality bone. In the eroded E2 type glenoid, this is located postero-superiorly encompassing two-thirds of the glenoid's surface and can be managed by dialing a full wedge augmented baseplate postero-superiorly.

Summary for Lay Audience

Improving the success of modern reverse shoulder replacements depends on proper attachment of the baseplate, a component of the shoulder replacement system that is in direct contact with bone. A biomechanical investigation using human cadavers examined how peripheral screw position and orientation affect baseplate fixation in normal glenoids that contain no bone loss. The results show no statistically significant difference between screw position (p=.60) or orientation (p=.20). In a subsequent study to determine best management in baseplate fixation when using a glenoid with bone erosion, a computer-model was used to assess the erosion in the so called E2 type glenoid. In the E2 type glenoid, erosion was found to be oriented upper left corner (in a right shoulder) and covering an average of 66% of the surface area of the glenoid. Overall, these findings suggest that surgeons may aim peripheral screws into the best quality bone. In the eroded

E2 type glenoid, this is located in the upper left corner, encompassing the majority of the glenoid's surface.

Keywords

Reverse Shoulder Arthroplasty; Baseplate Fixation; Micromotion; Screw Orientation; Locking; Compression; Glenoid; E2; Cuff Tear Arthropathy; Augmented Implants; BIO-RSA; Bone Loss

Co-Authorship Statement

Chapter 1:
Sole Author: Sejla Abdic
Manuscript Review: James A. Johnson, George S. Athwal

Chapter 2:
Study Design: Sejla Abdic, Jason Lockhart, James A. Johnson, George S. Athwal
Specimen Preparation: Sejla Abdic, Naser Alnusif
Data Collection: Sejla Abdic, Jason Lockhart
Data Analysis: Sejla Abdic, Jason Lockhart
Statistical Analysis: Sejla Abdic
Manuscript Preparation: Sejla Abdic
Manuscript Review: Jason Lockhart, James A. Johnson, George S. Athwal

Chapter 3:
Study Design: Sejla Abdic, Nikolas Knowles, James A. Johnson, George S. Athwal
Data Collection: Sejla Abdic
Data Analysis: Sejla Abdic
Statistical Analysis: Sejla Abdic
Manuscript Preparation: Sejla Abdic
Manuscript Review: Nikolas Knowles, James A. Johnson, George S. Athwal

Chapter 4:
Sole Author: Sejla Abdic
Manuscript Review: James A. Johnson, George S. Athwal

Acknowledgments

Primarily, my greatest thanks go to my mentor and friend, Dr. Philipp Moroder, who was the first to give me an opportunity to prove myself in the field of orthopaedic research. You believed in me from the beginning. Your expectations are high, and I always view them as coming from a place of support and a platform for continuous self-improvement.

My thesis is born from your kind recommendation to Dr. George Athwal, a genius in his field.

Dr. Athwal, my primary supervisor, thank you so much for taking me on as your student. I truly admire your professionalism and hard, dedicated work ethic. You are a man of your word and I feel honored to have the opportunity to learn from you. You surround yourself with the best in their field, and Dr. James Johnson is no exception.

Dr. Johnson, my second supervisor, I appreciate your kindness, your ongoing support and most importantly, your professional input in the development of this thesis. You are greatly appreciated and well-liked by all your students including me.

Many thanks go to everyone at the HULC lab, who I have had an opportunity to work with.

Table of Contents

List of Tables

List of Figures

Chapter 1

1 Introduction

OVERVIEW

This thesis explores strategies for improving baseplate fixation in reverse shoulder arthroplasty by first examining peripheral screw placement and orientation in non-eroded glenoids and subsequently quantifying the erosion pattern in the E2 type eroded glenoid to investigate its best surgical management with the previously gained results.

In this chapter, the pertinent anatomy of the shoulder joint and the concept of cuff tear arthropathy are reviewed. In addition, an overview of surgical management options with a focus on baseplate loosening and methods of fixation are introduced.

At the end of the chapter, the rationale, objectives, and hypotheses of this thesis are outlined.

1.1 The Shoulder

The human shoulder complex is the most versatile and mobile joint in the body with the largest range of motion of any joint[1,2]. The facilitators of this large range of motion are four articulations, the glenohumeral, sternoclavicular, acromioclavicular, and scapulothoracic joints. While all are concomitantly involved in the overall function of the shoulder complex, the glenohumeral joint along with its osseous anatomy and musculature will be the primary focus of this work. Its articulation is described as a synovial 'ball and socket' type joint, whereby the ball, the humeral head, rotates within the socket, the glenoid fossa, at a range of motion that includes three degrees of freedom. These include abduction and adduction, internal and external rotation, flexion and extension. This impressively versatile humeral orientation in a healthy shoulder allows the human arm to span a space larger than a hemisphere[3].

This large range of motion makes the glenohumeral joint inherently unstable, meaning it may lead to dislocation of the humeral head from the glenoid resulting in subsequent impingement and/or injury. In addition, the anatomic features of the large humeral head against the small and shallow glenoid fossa, produce a disproportionate congruency between the two and predispose the joint to further instability. Thus, stability of the glenohumeral joint is primarily facilitated by the synchronous interplay between passive and active structures within the joint, which consist of capsuloligamentous tissues and musculature, respectively. Healthy shoulder biomechanics are the result of a cooperative function of these aforementioned anatomic structures and the injury or disease of any of these components results in sub-optimal joint functioning[4].

In order to fully appreciate the biomechanical aspects of the shoulder, following is an introduction into the three components that contribute to the overall shoulder joint functioning, (i) the osseous components, (ii) the passive soft tissues, and (iii) the active musculature.

1.1.1 Osseous Components

The shoulder involves a total of three bones; the scapula, the clavicle, and the humerus (Figure 1-1), while the glenohumeral joint, the focus of this work, requires the understanding of the interaction between the humeral head and the glenoid, located laterally on the scapula.

The glenoid fossa is pear shaped with a shallow concave curvature, while the relatively large humeral head fits only partially and disproportionately onto its surface. In fact, only one third to one quarter of the humeral head fits onto the surface of the glenoid fossa[5–7], meaning that only part of the humeral head is in contact with the glenoid cavity at any given position of the glenohumeral joint[8]. This lack of congruency between the humeral head and the glenoid is a large contributor to the inherent instability of the joint.

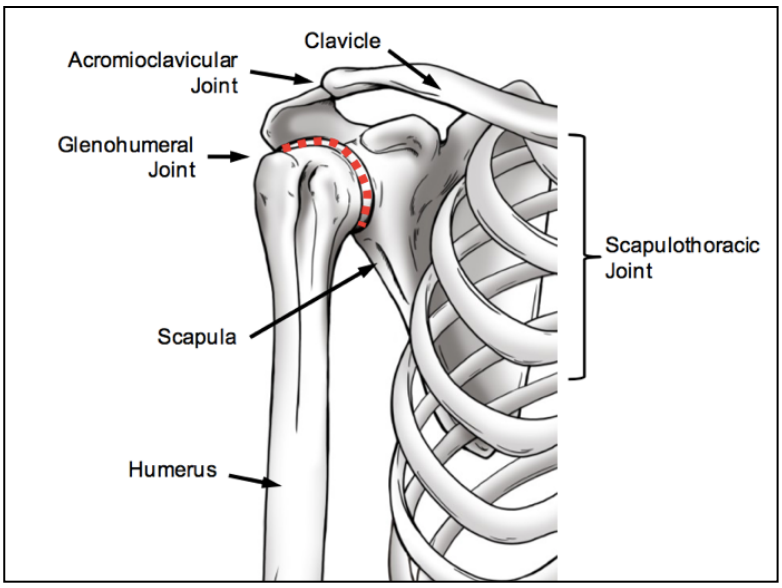

Figure 1-1: Basic shoulder anatomy – a simplified illustration of the glenohumeral joint.
The large convex head of the humerus fits only partially onto the glenoid, the lateral articulating surface of the scapula. Together, they form the glenohumeral joint (red dotted line). (Image retrieved from Langohr[9])

Healthy glenohumeral joint mechanics are reliant on many factors inherent to the scapula and the glenoid. Any abnormalities or defects that may be present can negatively affect glenoid morphology and overall shoulder stability and health. A crucial measure of glenoid characteristics is its version and inclination (Figure 1-2). Version (retroversion and anteversion) of the glenoid is measured in the axial plane and inclination (superior inclination and inferior inclination) is measured in the coronal plane. While the scapula sits on the posterior thorax with its glenoid oriented in an anterior tilt, the glenoid is actually retroverted with respect to its scapula. Though findings in the literature vary slightly, consensus among orthopedic surgeons is that the glenoid is retroverted and tilted superiorly[6].

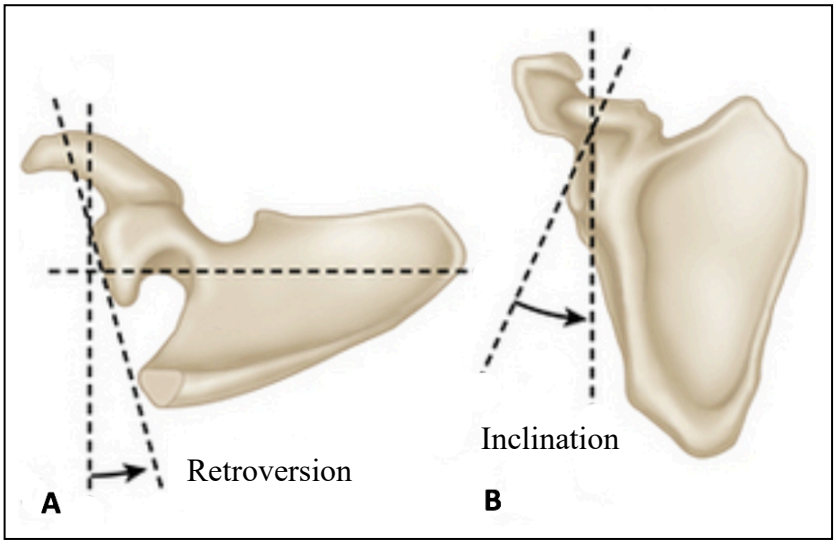

Figure 1-2: Glenoid version and inclination.
A: Superior view of a scapula. Glenoid version (anteversion/retroversion) is measured in the axial plane. B: Anterior view of a scapula. Glenoid inclination is measured in the coronal plane.
(Image retrieved from Lee[10])

1.1.2 Passive Soft Tissues

One mechanism involved in providing stability to the humeral head on the glenoid fossa both at rest and during movement is the glenohumeral joint capsule. The glenoid labrum, a fibrocartilaginous structure attached around the glenoid rim, and several surrounding ligaments such as the glenohumeral joint ligaments and coracohumeral ligaments are

additional supporters of stability. This is accomplished via a passive mechanism of stability, limiting mobility to a predetermined range of motion based on individual stiffness or laxity of such ligamentous structures.

In a healthy shoulder, stabilization of the humeral head within the glenoid is achieved through a coordinated, synchronous interplay between these capsuloligamentous passive structures and the surrounding musculature of the shoulder acting as active stabilizers.

1.1.3 Active Musculature

Healthy shoulder muscles are involved in both mobility and stability of the glenohumeral joint. They consist of the supraspinatus muscle, infraspinatus muscle, teres minor and subscapularis muscle, conjunctively termed the rotator cuff (Figure 1-3). Through active contraction, the rotator cuff maintains a compressive force onto the glenohumeral joint mechanism. A well-balanced strength of each muscle is jointly responsible for adding equal constraint to the humeral head, thereby, centralizing it onto the glenoid surface.

Damage to the rotator cuff can occur due to trauma, overuse, or bony deformities, and the incidence of injury increases with increasing age[11–13].

While the mechanism of injury to the rotator cuff can be different, the ultimate result is a tear in the musculature or tendons that attach the muscles to their respective bony insertions. Any such tear results in long-term muscular imbalance of the rotator cuff, leading to what was first termed by Neer et al.[14] as classic cuff tear arthropathy.

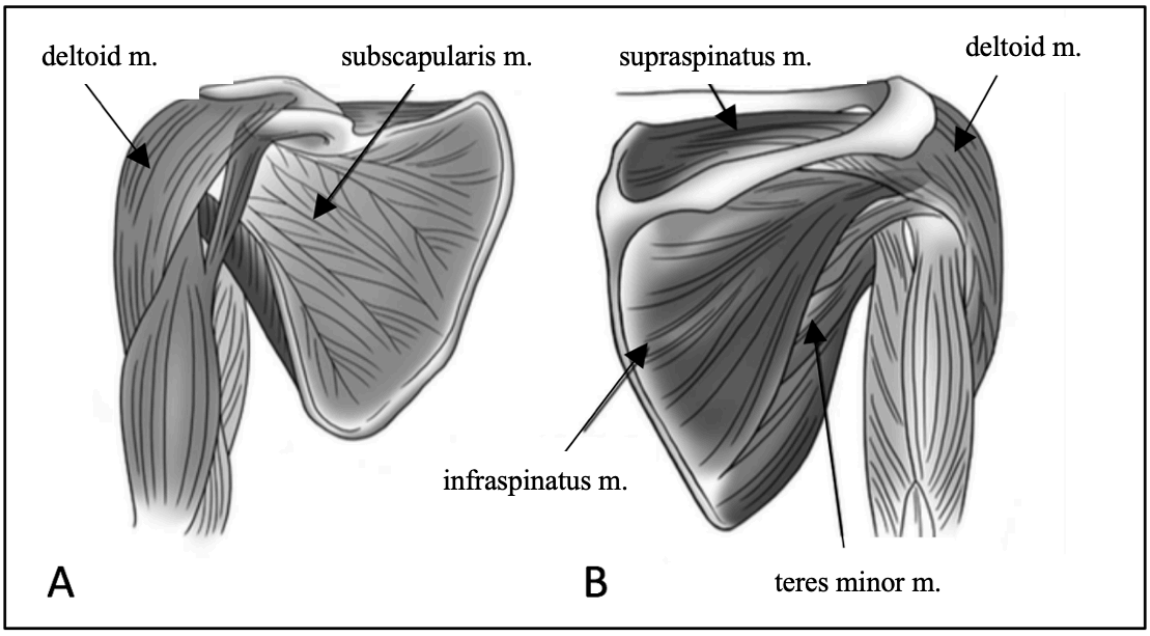

Figure 1-3: **The rotator cuff of the shoulder.**
The subscapularis muscle on the ventral side (A), supraspinatus muscle, infraspinatus muscle and teres minor muscle on the dorsal side (B) of the shoulder blade, collectively make up the rotator cuff. The deltoid muscle, also seen in this image, is an important additional stabilizer of the glenohumeral joint. (Image retrieved from Langohr[9])

1.2 Cuff Tear Arthropathy

In the early 1980s, Neer et al.[14,15] began using the term 'rotator cuff arthropathy' for conditions of the glenohumeral joint to describe arthritic changes and degeneration as a result of massive postero-superior rotator cuff tears. While any of the rotator cuff structures may tear, it is in particular the supraspinatus muscle that tears most frequently[1,34], and in conjunction with infraspinatus tears, the term postero-superior rotator cuff tear (referring to the anatomic location on the scapula of the respective muscles) is used.

Typically, minor rotator cuff tears can be managed non-operatively in some patient populations, but treatment algorithms can vary from patient to patient depending on the mechanism of injury and the extent of musculo-ligamentous involvement. Non-operative treatment for minor rotator cuff tears includes options such as rest, physiotherapy,

NSAIDs and intra-articular corticosteroid injections, often taking precedence to any operative treatment considerations.

Failure to respond to non-operative options and acute traumatic injury to the rotator cuff in active young patients can be treated with surgical tendon repair as a secondary option. This is often undertaken either arthroscopically[18], a minor invasive approach to the site of injury, or may include open surgical repair for better visualization[19] to adequately restore the balancing forces provided by the rotator cuff and to ensure appropriate glenohumeral stability and function of the shoulder joint.

Degenerative and chronic disease of the rotator cuff is often associated with increased age[20–23] and often presents asymptomatically[24], but is the most debilitating condition of all.

1.2.1 Chronic Irreparable Rotator Cuff Tears

Cadaveric[20,21,25,26] and in vivo imaging studies[27,28] have been conducted to better understand the prevalence of chronic rotator cuff disease, but true prevalence remains unclear as reported numbers are largely variable.

Chronic rotator cuff disease often has an insidious onset however, acute exacerbations of chronic disease may present as night pain and difficulty sleeping on the affected side. Patients most often present with pain on active range of motion especially during overhead activities, though passive movement on physical exam is generally tolerated. Subsequent presentation involves weakness and complete loss of range of motion beyond 90°-130° overhead. This presents as highly debilitating pain in every-day activities, limiting patients' quality of life significantly. Actions such as reaching into overhead kitchen cupboards, washing or brushing one's hair, or household cleaning may become limited or impossible.

Diagnostic investigations of chronic rotator cuff tears include x-ray imaging of the shoulder in antero-posterior view, showing a high-riding humerus relative to the glenoid. This is a pathognomonic radiographic sign for large rotator cuff tears and severe chronic

tendinopathy. MRI imaging in coronal, sagittal oblique and axial orientations can be useful for assessing partial versus full tear tendinopathy.

Full thickness tendon tears of the rotator cuff, when left untreated, may slowly lead to muscle retraction and subsequent fatty infiltration of individual muscles combined with muscle atrophy[29] through a mechanism that is still not fully understood. This fatty progression can render the rotator cuff as 'irreparable'. Fatty infiltration of the rotator cuff has been shown to be a poor prognostic factor for surgical repair of the cuff tendons [30–32]. Thus, in clinical practice, a classification of fatty infiltration of the rotator cuff termed the Goutallier classification serves as a prognostic tool, assisting surgeons in anticipating potential benefits or risks to various interventions in irreparable or massive rotator cuff tears.

1.2.2 Fatty Infiltration of the Rotator Cuff

Originally, fatty infiltration has been characterized by areas of decreased radiodensity in non-contrast CT scans, however, today T1-weighted MRI imaging is best used to visualize the changes. The original Goutallier classification using CT-scan imaging - the method of choice used in this study - ranges from Grade 0 (normal muscle, without fatty streaks), Grade 1 (some fatty streaks visible), Grade 2 (more muscle than fat), Grade 3 (equal amounts of fat and muscle) to Grade 4 (more fat than muscle). Figure 1-4 depicts a CT scan in sagittal oblique view (also termed 'Y-view') of a right shoulder. In this view, each rotator cuff muscle may be assessed for their respective grade of fatty infiltration.

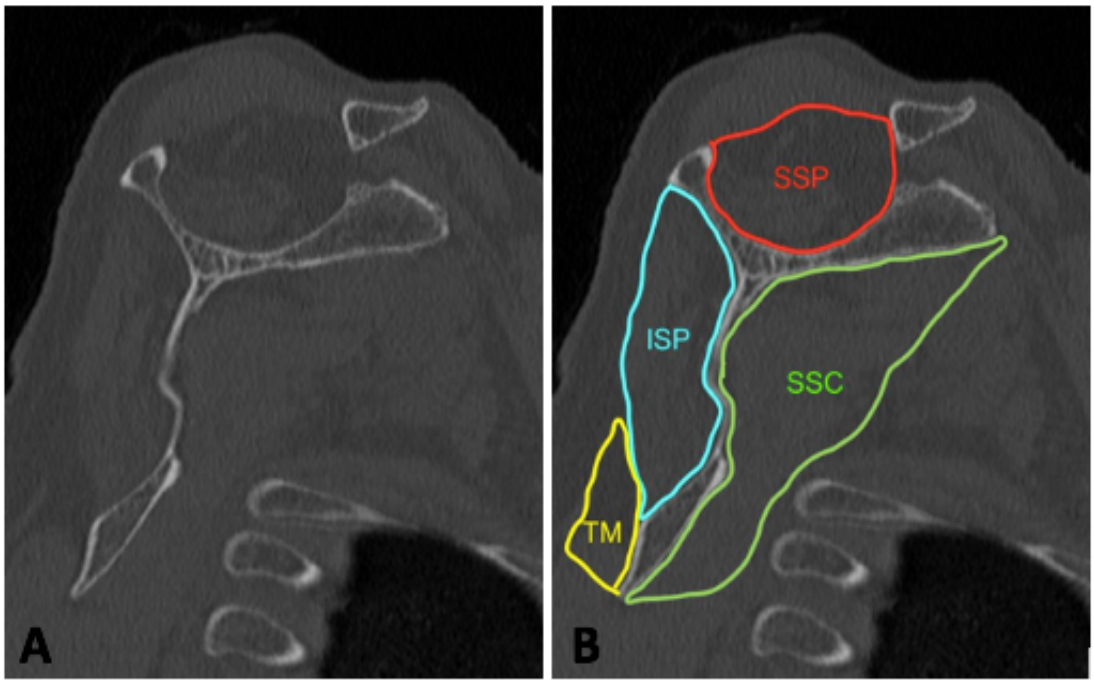

Figure 1-4: **CT scan in sagittal oblique view ('Y-view') of a right shoulder.**
This view allows for assessment of the degree of fatty infiltration of each of the four rotator cuff muscles. B: Anatomic location of SSP = supraspinatus, ISP = infraspinatus, TM = teres minor, SSC = subscapularis and dimensions in a normal, non-fatty infiltrated, state.
(S. Abdic, 2018)

Chronic damage to the muscles of the rotator cuff leads to an imbalance of normal shoulder kinematics and concomitant chronic morphologic changes of the humeral head and the glenoid, consistent with glenohumeral osteoarthritis. To date, it is unclear, whether osteoarthritis precedes rotator cuff damage, or vice versa. Regardless, osteoarthritis of the shoulder is the primary indication for shoulder arthroplasty and in the case of a non-functional rotator cuff, reverse shoulder arthroplasty is the preferred method of treatment.

1.2.3 Glenoid Bone Erosion

Chronic damage to the muscles of the rotator cuff leads to an imbalance of normal shoulder kinematics and concomitant chronic morphologic changes of the humeral head and the glenoid, consistent with glenohumeral osteoarthritis. To date, it is unclear,

whether osteoarthritis precedes rotator cuff damage, or vice versa. What we understand, however, is that over time, patients with rotator cuff arthropathy develop glenoid bone erosion at an incidence close to 40%[33,34]. Though bone erosion can occur anywhere on the glenoid, it most frequently comprises the posterior and superior region of the glenoid surface. Approximately 9% of patients with cuff tear arthropathy demonstrate superior erosion.

In 1999, Walch et al[35]. began classifying glenoid erosion in hopes of gaining prognostic insight into erosion patterns of glenoids in primary osteoarthritis. They examined 113 CT scans of arthritic shoulders and developed a classification method according to the pattern and severity of glenoid erosion, as well as version. In 2016, Bercik et al. proposed a modified classification system to the original Walch classification[36] (Figure 1-5). In type A glenoids, the humeral head is centered on the glenoid that either contains minor (type A1) or major (type A2) erosion. In their cohort, this was also the most frequently encountered type at close to 60%. In type B glenoids, there is posterior subluxation of the humeral head present, with type B1 containing no erosion and type B2 demonstrating marked posterior erosion, revealing a biconcave glenoid. Type C glenoids are defined by severe erosion, such that the retroversion is greater than 25°, a feature that makes them 'hypoplastic'. Type B3 are defined as monoconcave with retroversion of more than 15°. Type C glenoids demonstrate at least 25° retroversion regardless of erosion and in type D glenoids there is anteversion with/without anterior subluxation present.

In the setting of massive irreparable rotator cuff tears and rotator cuff arthropathy, Favard et al.[37] created a classification system to describe different types of superior glenoid wear due to humeral head subluxation. In the schematic representation of erosion seen in Figure 1-6, E0 type represents a normal glenoid. E1 type may be seen as similar to Walch's A1 type with concentric central wear. Favard's type E2 glenoids, and the focus of this study, is defined as a superiorly eroded glenoid with the erosion not extending towards the inferior glenoid rim. E3 type glenoids are defined as superiorly eroded glenoids with no remaining articular bone left, thus, containing exaggerated superior inclination. Type E4 glenoids demonstrate erosion that is predominantly located in the inferior part of the glenoid.

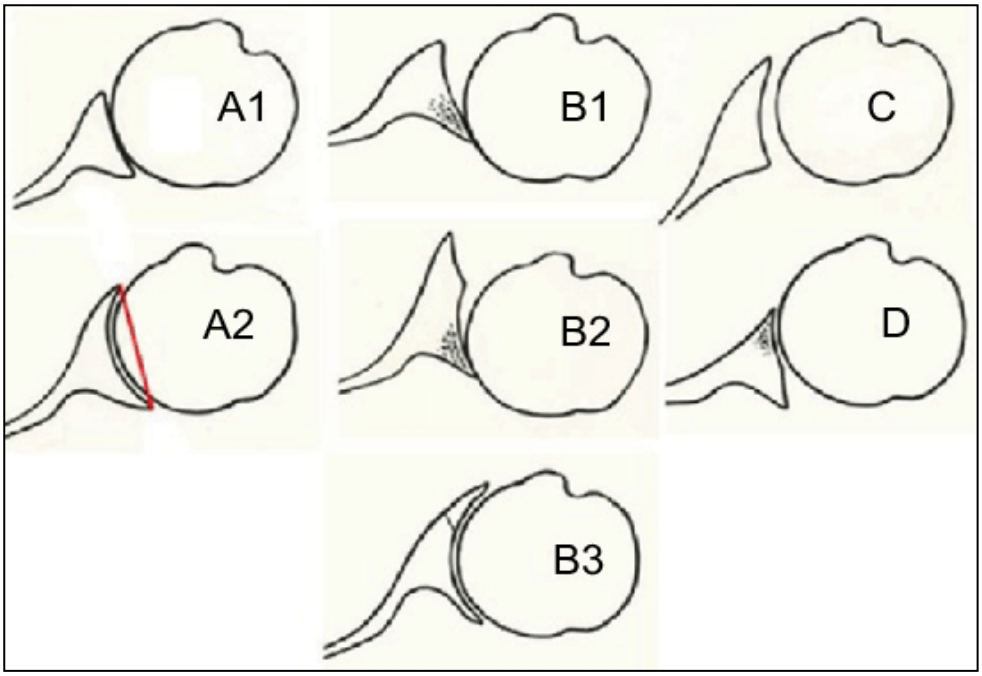

Figure 1-5: **Walch type classfication of glenoid erosion in arthritic shoulders.** *Type A1: mild glenoid erosion, humeral head is centered. Type A2: major glenoid erosion, with centered humeral head. Type B1: no erosion, but posterior subluxation of the humeral head. Type B2: biconcave glenoid with posterior erosion. Type B3: monoconcave with >15° retroversion. Type C: at least 25° retroversion. Type D: anteversion with/without anterior subluxation. (Image retrieved from Bercik et al.*[36]*)*

Currently, the understanding of the progression of superior glenoid wear due to rotator cuff arthropathy is that there exists an unopposed action of the deltoid muscle on the humerus in the context of a weak rotator cuff, which would normally help constrain the humeral head centrally onto the glenoid. The deltoid muscle's effect on the humerus is in a superior direction, leading to superior migration of the humeral head in chronic rotator cuff disease. This superior migration of the humeral head can easily be seen in radiographic imaging (Figure 1-7), adding to the progression of superior glenoid erosion and the development of an E2 type glenoid.

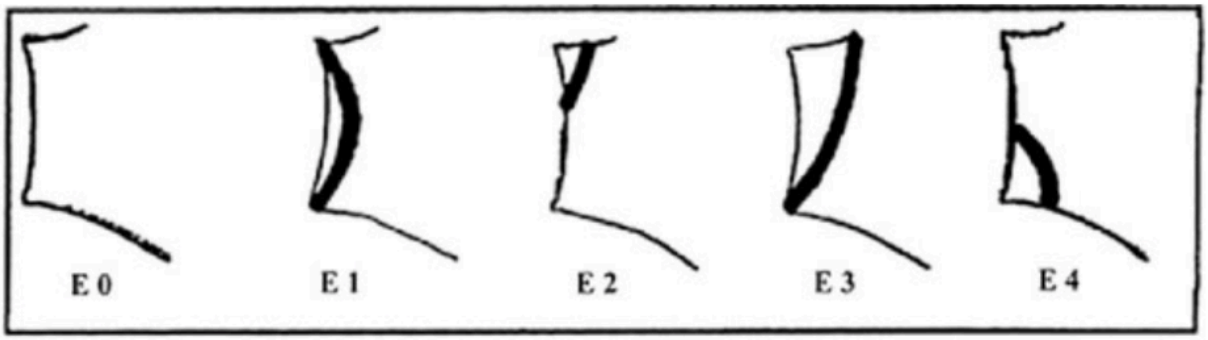

Figure 1-6: **Favard type classification of glenoid erosion in rotator cuff arthropathy.**
Type E0: normal glenoid. Type E1: contains concentric wear. Type E2: superior wear with normal inferior rim. Type E3: superior erosion with increased superior tilt. Type E4: erosion located at the inferior part of the glenoid. (Image retrieved from Levigne et al.[38]*)*

Osteoarthritis of the shoulder is the primary indication for shoulder arthroplasty and in the case of a non-functional rotator cuff, reverse shoulder arthroplasty is the preferred method of treatment.

Following is a short introduction into treatment methods that address both osteoarthritis and rotator cuff arthropathy with concurrent glenoid bone loss including a brief explanation of the methods and devices used.

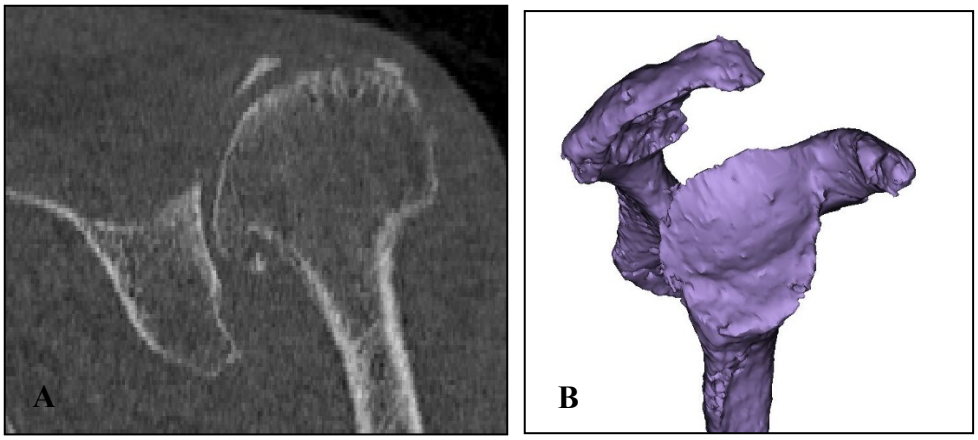

Figure 1-7: **Superior glenoid erosion of the E2 type.**
(A) A 2D coronal CT scan view of a left shoulder demonstrating a superiorly eroded E2 type glenoid. (B) A sagittal, en-face view of a right CT reconstructed 3D scapula, containing an E2 glenoid with supero-posterior erosion. (S. Abdic, 2018)

1.3 Shoulder Arthroplasty

Total shoulder arthroplasty (TSA) is an orthopaedic surgical procedure that replaces the articular surfaces of the humeral head and the glenoid. It is successful in addressing patient's shoulder pain and loss of function due to bone-on-bone contact in the setting of glenohumeral osteoarthritis. In this procedure, the humeral head is resected and replaced by a spherical metal component, while a polyethylene insert is attached to the glenoid surface. Though this procedure has good patient outcomes overall, it is rendered unsatisfactory in patients with a deficient rotator cuff. Patients with massive cuff tears are unable to achieve the range of motion in their shoulder joint that is required to act out activities of daily living. Thus, total shoulder arthroplasty does not address this loss adequately.

Reverse total shoulder arthroplasty (RTSA) is a method that addresses this problem. It was first described by Grammont et al[37]. in the 1980's as a treatment for patients with cuff tear arthropathy. This surgical procedure changes the anatomy of the glenohumeral joint (Figure 1-8) in that it reverses the polarity of the 'ball and socket' as we know it.

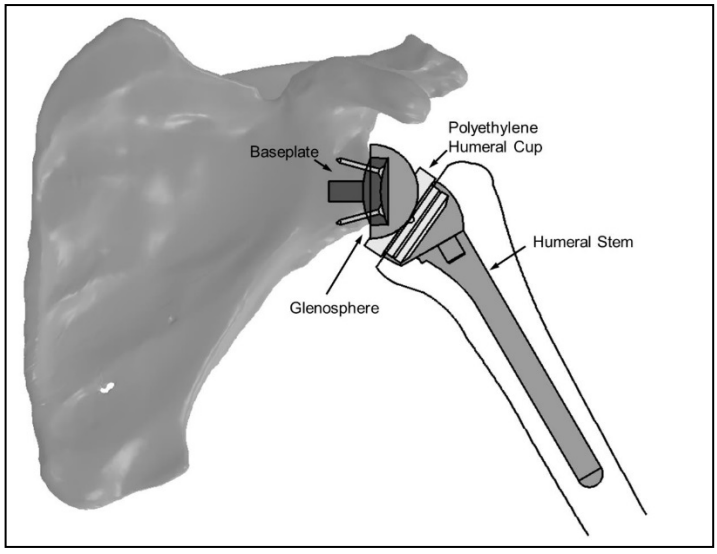

Figure 1-8: A reverse total shoulder arthroplasty prosthesis with its corresponding components.
The anatomy of the 'ball and socket' in the glenohumeral joint is reversed, consequently changing the joint kinematics of the shoulder.
(Image retrieved from Langohr[9])

1.3.1 Reverse Total Shoulder Arthroplasty

In reverse total shoulder arthroplasty, a 'ball' component termed the glenosphere is placed onto the glenoid surface, while the humeral head is replaced by a 'socket' polyethylene cup (Figure 8). This reversal provides mechanical advantage in that it medializes the center of joint rotation of the native glenohumeral joint. The humeral stem of the reverse prosthesis is inserted into the intramedullary canal of the humerus, which serves as a fixation for the humeral polyethylene cup. Stemless designs to enhance load transfer to bone are now gaining more popularity. On the glenoid side, the baseplate anchors the glenosphere into place and its fixation is facilitated via a central peg and peripheral screws that are geared into the glenoid vault of the scapula.

This concept of anatomic reversal provides a longer moment arm upon which the deltoid muscle can act. Thus, the deltoid force required to achieve mobility of the joint is reduced. This compensates for the loss of the rotator cuff.

As implant designs continue to be modernized and improved, there are marked advancements in surgical techniques and indications for RTSA. This is still a relatively new operation in orthopaedics and a risk with the use of such a device is implant failure due to aseptic loosening. Loosening can occur due to many reasons that increase shear loading and moments of the device. However, improper placement of the implant peri-operatively, is an important aspect that needs to be addressed.

1.3.2 Aseptic Loosening in RTSA

The reverse total shoulder arthroplasty design contains a humeral component as well as a glenosphere that is affixed to the glenoid bone via a baseplate[39], which is the sole component in direct contact with the scapular bone. Adequate glenoid baseplate fixation is critical for ensuring the shoulder replacement's longevity and it is most commonly the baseplate that is the source of early aseptic loosening of the system[40–42]. This is a serious complication of RTSA that may require revision surgery. The true incidence of glenoid loosening varies in the literature and has been reported to reach up to 12%[43,44]. Over time, several improvements in surgical technique as well as implant design have assisted in reducing baseplate failures[45]. These include developing an understanding of the

significance of baseplate tilt[46–48], consideration of screw positioning and placement[34,45,49–52], glenoid reaming techniques[42], the use of peripheral screws for fixation[53], baseplate morphology and position[52,54,55], and the introduction of bone ingrowth technologies[55].

1.3.3 Baseplate Fixation Methods

Over the past decade and a half, baseplate failure rates have been improved by advancements in surgical technique as well as implant design. Of those, screw fixation methods have been noted to be the most crucial aspect involved in enhancing fixation[52,54,56]. The introduction of peripheral locking screws is one key improvement in surgical technique that helped improve glenoid baseplate fixation. Harman et al.[57] first revealed that locking screws significantly strengthened baseplate fixation while minimizing micromotion between the baseplate and glenoid bone. Clinical studies conducted by Frankle et al. reported an 11% baseplate failure rate when 3.5-mm non-locking screws were used[58], but a decrease in failure rate to 0% was observed in a 5-year follow-up using the same implant with 5.0-mm peripheral locking screws[59]. Ultimately, this method of peripheral screw fixation has been adopted by many surgeons.

There are, however, situations in the operating room that warrant the use of non-locking peripheral screws, because using all four peripheral locking screws may either not be feasible or may not represent a surgical preference. Such scenarios may include limited bone stock that does not allow for minimal bone capture by the screw or result in a prominent screw; or situations in which a larger locking screw may be disadvantageous, potentially raising stress levels that may lead to acromial stress fractures[60]. In addition, cases in which a surgeon may prefer using non-locking screws include situations in which additional glenoid baseplate compression is desirable, a key mechanical property of non-locking screws.

Historically, a hybrid configuration of locking and non-locking screws has been successfully used in locked plate osteosynthesis. This method is biomechanically similar while providing the added benefits of compression while aiding in reduction[61–64]. Formaini et al.[65] tested the concept of hybrid configurations of locked and unlocked peripheral screws in glenoid baseplate fixation in polyurethane bone substitute models

and found acceptable baseplate fixation that maintained micromotion below the necessary threshold for bony ingrowth.

In the literature, several authors have examined the effect of the number of screws as well as their positioning and arrangement on glenoid baseplate fixation, but with mixed results[48,54,66–68].

1.3.4 Augmented RTSA Baseplates

A challenging situation that may be encountered during reverse shoulder arthroplasty is the presence of glenoid erosion due to rotator cuff arthropathy. Incorrect positioning of the glenoid baseplate due to deficient bone can result in residual tilt of the components and may negatively impact long-term component stability. For example, in the case of an superiorly eroded E2 glenoid, superior tilt of the baseplate has been associated with an increased risk of aseptic loosening and instability[46,47]. Surgical techniques that address glenoid erosion in RTSA include asymmetric reaming, bone grafting, or the use of augmented baseplates[69].

Implants that are designed to address bony erosion are referred to as augmented baseplates and there is a variety of commercially available designs (Figure 1-9).

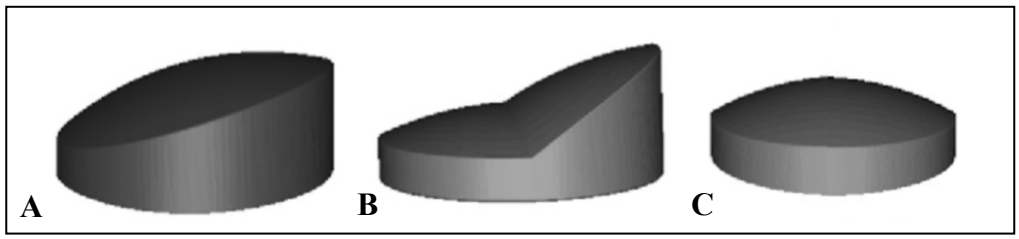

Figure 1-9: Simplified view of augmented baseplate designs.
Full-wedge (A), half-wedge (B), and standard flat (C) designs of glenoid baseplates to facilitate filling of bony defects. Patient-matched designs (not shown) employ a standard (flat) baseplate with autografted bone below the baseplate to fill bony defects of the glenoid.
(S. Abdic, 2018)

1.4 Motivation

Reverse total shoulder arthroplasty (RTSA) remains a relatively new procedure in shoulder surgery, and the overall longevity of a RTSA prosthesis can be significantly compromised by a range of complications including hardware failure. Although not common, one such catastrophic complication is early baseplate migration and failure[40,53,68]. This is primarily attributed to low quality initial fixation of the baseplate during surgery and low adaptation of the baseplate to a patient's native bone.

Previous literature includes studies that investigated different approaches that lead to enhanced baseplate fixation in RTSA, including considerations of baseplate tilt[47,48,70], glenoid reaming techniques[42], screw positioning and placement[34,49–51,67], baseplate morphology and position[41,52] as well as bone ingrowth technologies[41]. Of these, the use of screw fixation is ubiquitous among all glenoid baseplate designs. Additionally, apart from a number of remaining concepts that yet need to be answered, overall knowledge pertaining to improving baseplate fixation in the non-eroded, anatomical glenoid is well established in the literature.

In the presence of glenoid erosion and pathoanatomical changes of the glenoid encountered during RTSA procedures, a highly challenging situation arises with regards to adequate fixation of the baseplate, even for the most experienced surgeon. Significant paucity of knowledge exists pertaining to patterns of glenoid erosion, the progression of erosion over time and its best surgical management in RTSA.

Therefore, the motivation behind the studies included in this thesis lays in the desire to answer fundamental questions pertaining to improvement in glenoid baseplate fixation in RTSA. In specific, the approach herein is to fill a gap of knowledge pertaining to baseplate fixation in the well-studied 'non-eroded glenoid' (Chapter 2) and attempts to reconcile this information by extrapolating the findings to the surgical management of the less studied 'eroded glenoid' (Chapter 3).

1.5 Objectives and Hypotheses

Specific to each chapter included in this thesis, the objectives are as follows:

1. To determine whether there is a quantitative difference in the quality of time-zero baseplate fixation between two different configurations of locking screw position and orientation in an anatomically normal glenoid. (Chapter 2)

2. To quantify glenoid erosion and orientation in the E2 glenoid. (Chapter 3)

3. To examine four augmented reverse baseplate designs in the management of E2 erosions (standard, half-wedge, full-wedge, and patient-matched/BIO-RSA) with regards to the amount of bone volume removal necessary for proper seating of the baseplate. (Chapter 3)

4. To ascertain the amount of fatty infiltration of the rotator cuff in the E2 eroded glenoid. (Chapter 3)

Specific to each chapter included in this thesis, the hypotheses are as follows:

1. Eccentric loading along the supero-inferior axis of the glenoid would produce better baseplate fixation in the configuration containing locking screws in the supero-inferior (SI) screw holes because of the fixed angle mechanical characteristic of locking screws.

2. A divergent screw orientation would outperform a parallel screw insertion into the glenoid vault in terms of baseplate micromotion and, thus, stability.

3. In the E2 eroded glenoid, erosion does not occur purely superiorly but is oriented in a predictable posterosuperior direction.

4. There is significant rotator cuff fatty infiltration along the supero-posterior rotator cuff in an E2 eroded glenoid and subscapularis muscle fatty infiltration may affect overall erosion orientation.

5. There is a significant difference in the amount of bone volume removal necessary between different augmented reverse baseplate designs in the management of E2 erosions.

1.6 Thesis Overview

This thesis answers some questions that remain pertaining to enhancing glenoid baseplate fixation in RTSA in non-eroded glenoids and adds to the groundwork for further research into the quantification of glenoid erosions including their best surgical management with regards to baseplate fixation in RTSA.

In specific, Chapter 2 presents comparative data of an *in vitro* cadaver based study on RTSA glenoid baseplate fixation in the non-eroded glenoid by assessing baseplate micromotion in different arrangements of peripheral screw position and orientation.

Chapter 3 first elucidates detailed computer software quantification and orientation of pathoanatomic glenoid erosion in the E2 type glenoid. Subsequently, fatty infiltration around the E2 glenoid is quantified and ultimately, the best surgical management of an E2 type eroded glenoid is elucidated by comparing different augmented baseplate designs.

Chapter 4 offers a final overview and discussion of the findings and potential future directions in the field.

Chapter 2

2 Glenoid Baseplate Screw Fixation in Reverse Shoulder Arthroplasty: Does Locking Screw Position and Orientation Matter?

OVERVIEW

In a reverse total shoulder arthroplasty (RTSA) prosthesis, the longevity of the construct can be compromised by glenoid baseplate loosening. A circular baseplate design can be secured with supero-inferior locking screws and antero-posterior compression screws or vice versa.

This chapter examines peripheral screw position and peripheral screw orientation in a biomechanical cadaveric model to determine quantitative differences in baseplate micromotion and adds to improving overall baseplate fixation in RTSA in a non-eroded glenoid[a].

a) A version of this work has been accepted for publication: Abdic S, Lockhart J, Alnusif N, Johnson JA, Athwal GA. Glenoid Baseplate Screw Fixation in Reverse Shoulder Arthroplasty: Does Locking Screw Position and Orientation Matter? *Journal of Shoulder and Elbow Surgery, 2020 Aug 25*

2.1 Introduction

The biomechanical understanding of reverse total shoulder arthroplasty (RTSA) has seen significant advancements in the last decade, resulting in design optimizations, better patient outcomes and expanding indications. Despite this, complications after RTSA do occur and have been reported to range from 19% to 68%[40,66,71,72]. Although not common, one such catastrophic complication is early baseplate migration and failure[40,53,68]. This is most commonly caused by changes in biomechanical forces in the new glenohumeral joint seen after RTSA surgery. The results may be unpredictable stresses and excessive micromotion at the glenoid bone-baseplate interface, which may unfavorably affect baseplate stability and bone on-growth. Therefore, maximizing baseplate stability has been continuously investigated. Most notably, the scientific community has recognized different approaches that lead to enhanced baseplate fixation in RTSA, including considerations of baseplate tilt[47,48,70], glenoid reaming techniques[42], screw positioning and placement[34,49–51,67], baseplate morphology and position[41,52] as well as bone ingrowth technologies[41]. Of these, the use of screw fixation is ubiquitous among all glenoid baseplate designs. As such, optimization of screw orientation and configuration may lead to enhanced initial and potentially longer-term stability, which may translate to better bone on-growth or in-growth[49,52,54].

The purpose of this cadaveric biomechanical study was to gain comparative data on RTSA glenoid baseplate fixation by assessing baseplate micromotion in four arrangements of screw position and orientation. In specific, the aim was to compare the quality of baseplate fixation with locking screws in supero-inferior position compared to antero-posterior position, including a comparison of effect of parallel versus divergent screw orientation. The main objective was to determine whether there is a statistically significant quantitative difference in the quality of time-zero baseplate fixation between the resulting four locking screw configurations. We hypothesized, that eccentric loading along the supero-inferior axis would produce better baseplate fixation in the configuration containing locking screws in the supero-inferior (SI) screw holes because of the fixed angle mechanical characteristic of locking screws. Additionally, we hypothesized that a divergent screw orientation would outperform the parallel group, in

light of previous finite element studies reporting that screw divergence contributed to higher baseplate stability[73,74].

2.2 Methods

2.2.1 Specimen Characteristics

Ten paired (n=20 total, 64±7 years, range, 51-71 years) male fresh-frozen cadaveric shoulders were thawed overnight and the scapulae were disarticulated and dissected of all soft tissues. The denuded scapulae were potted in acrylic cement for stabilization during testing. Each cadaveric shoulder pair was randomly assigned to two different screw configuration patterns. One received locking screws in the conventional supero-inferior (SI) position and the other received locking screws in the experimental antero-posterior (AP) position. Compression screws were inserted in the remaining two screw holes in each screw configuration (Figure 2-1).

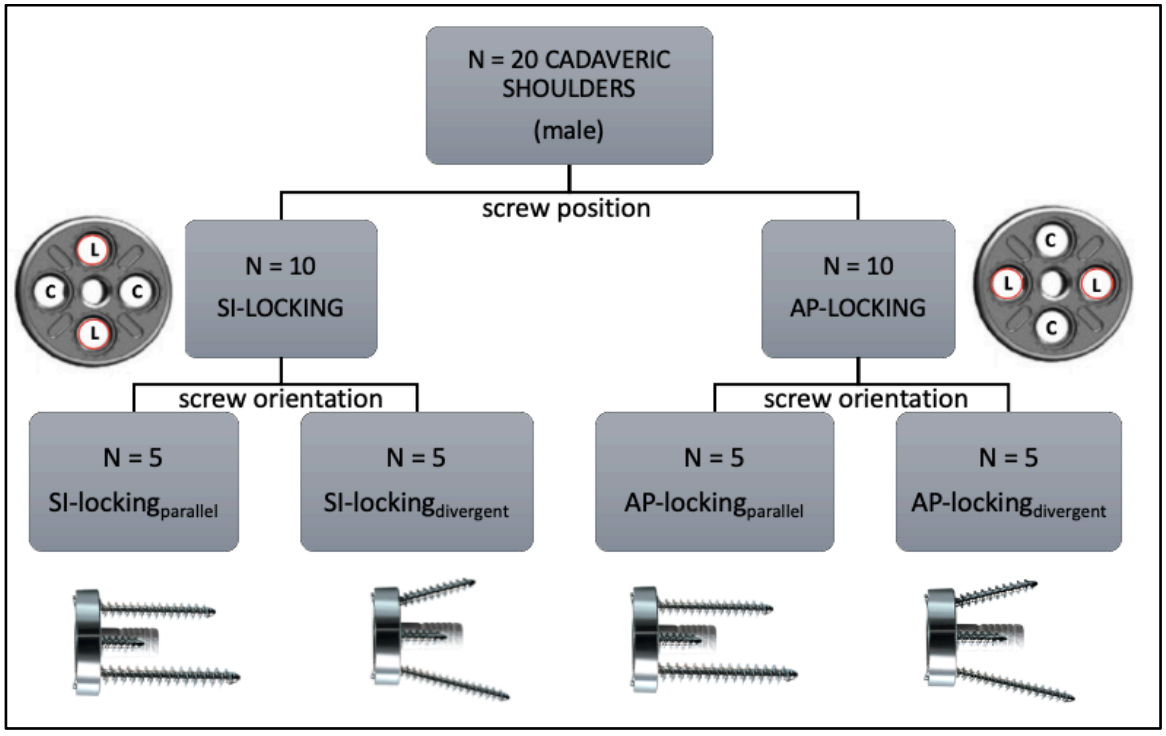

Figure 2-1: Study protocol.
The study protocol produced a total of four different groups (n=5 each) for comparison. L = locking screw, C = compression screw, SI = supero-inferior, AP = antero-posterior.

The randomization according to screw position yielded two groups of 10 cadaveric shoulders each, which were further subdivided according to screw orientation. One group was randomly assigned to a parallel screw orientation, entering the glenoid vault at 0° (or perpendicular to the glenoid baseplate's backside), while the other was comprised of supero-inferior screws oriented at a divergent angle of 15°. Ultimately, this resulted in four groups for comparison, each containing n=5 specimens: SI-locking$_{parallel}$, AP-locking$_{parallel}$, SI-locking$_{divergent}$, and AP-locking$_{divergent}$. The four groups were each comparable regarding average age; mean age was 64±8 years (range, 51-70 years) for the SI-locking$_{parallel}$ and AP-locking$_{parallel}$ groups, and 64±7 (range, 54-71) for the SI-locking$_{divergent}$ and AP-locking$_{divergent}$ groups. All screws were inserted bicortically in all groups.

The average bone density of the specimens was 923 ± 72 HU (Hounsfield units) and was calculated via a medical imaging software (Mimics® V. 17.0, Materialize, Leuven, BE) from computed tomography (CT) scans in digital imaging and communications in medicine (DICOM) format using multi-slice CT scanners with standard clinical settings (120 to 140 kVp, 512x512 resolution).

2.2.2 Surgical Procedure of Implantation

The implantation of the reverse total shoulder glenoid baseplate (29mm diameter, Aequalis^{TM} Reversed II Shoulder System, Wright Medical Group, Memphis, TN, USA) was conducted by a single fellowship trained orthopedic surgeon using the cannulated surgical glenoid preparation technique. At the first stage, a 2.5mm guide wire pin was inserted centrally and perpendicular to the glenoid at the 0° pin hole of a 29mm pin guide, by positioning the pin guide over the inferior edge of the glenoid. Once the guide pin was inserted, a cannulated circular reamer of 29mm diameter was used to create a flat glenoid surface for full seating of the baseplate (Figure 2-2). A 36mm peripheral reamer was used to remove excess bone to even the glenoid surface around the baseplate. The glenoid central hole was drilled using a 7.5mm diameter and 15mm length cannulated drill bit. Upon successful removal of the guide wire, the glenoid baseplate was impacted with a press fit of its 8mm diameter central post.

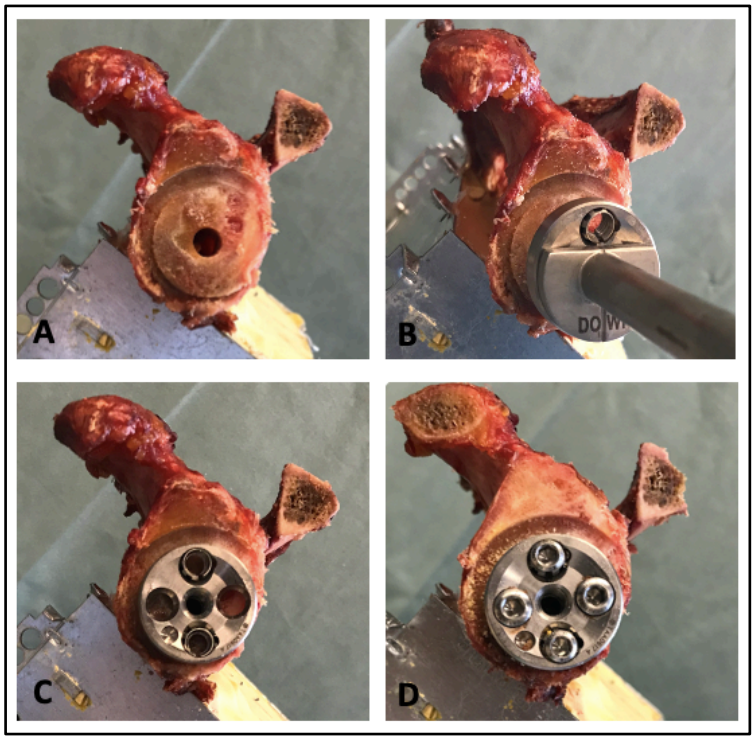

Figure 2-2: Baseplate implantation in a cadaveric scapula.
Implantation steps (A-C) of a 29mm diameter standard post baseplate. D: Final potted scapula-baseplate construct with locking screws supero-inferiorly and compression screws antero-posteriorly. Note: acromion and coracoid process were resected to avoid interference with axial loading of the baseplate.

During the defining step of baseplate impaction (Figure 2-B), the orientation of the locking screw holes was confirmed based on the randomization. Full seating of the baseplate onto glenoid bone was ensured by visually inspecting that the baseplate was flush with the prepared glenoid surface throughout, before the baseplate impactor was removed. Fixation of the glenoid baseplate occurred with the use of four 4.5mm self-tapping screws, consisting of two compression screws and two locking screws after drilling with the corresponding 3mm drill bit. To maximize compression of the baseplate to the glenoid, the compression screws were fully tightened prior to the locking screws using an alternate manual tightening technique.

The SI-locking group was subdivided into two separate groups, with one group containing neutral 0° (parallel) locking screw arrangement and the other group containing

a 15° divergent locking screw orientation. In each case, the screw orientation angle of the superior and inferior screws was controlled with the use of a goniometer. Their direction was maintained within the coronal plane and did not diverge in the transverse plane. Similarly, in the AP-locking group, the orientation of the supero-inferior compression screws was ensured with the use of a goniometer (Figure 2-D), at both 0° and 15° divergently. The final construct of the potted scapula with its implanted baseplate (Figure 2-D) required resection of the coracoid tip and/or part of the lateral acromion, in order to allow biomechanical testing, as indicated in the following steps.

2.2.3 Testing Protocol

Resistance of the glenoid baseplate to loosening was tested using relevant segments of the American Standard of Testing of Materials (ASTM)[75] for dynamic evaluation of glenoid loosening. It is assumed that glenoid component loosening occurs because of eccentric loading, often referred to as the rocking-horse phenomenon. This results in a combination of a compressive and bending moment load acting on the implant. As such, the test apparatus (Figure 2-3) imitated eccentric loading in the following way: a (4 mm thick) rigid plate was affixed to the glenoid via a central screw not extending into the glenoid bone. The rigid plate housed 3 linear variable differential transformers (0236-0000 LVDT; Trans-Tek, CT, USA) which were placed radially around the implant, at angles of 120°, 200°, and 240° relative to the supero-inferior axis. The LVDTs were used to create a coordinate system that defined 3 degrees of freedom (DOF) motion of the baseplate. Baseplate displacement, or micromotion, was computed at the superior and inferior edges of the implant by transforming the measured LVDT data to the edge of the baseplate using the known rigid position relationship between the LVDTs and baseplate. The primary outcome variable in this study was lift off, in micrometers (μm), of the baseplate edge that was opposite of the applied load.

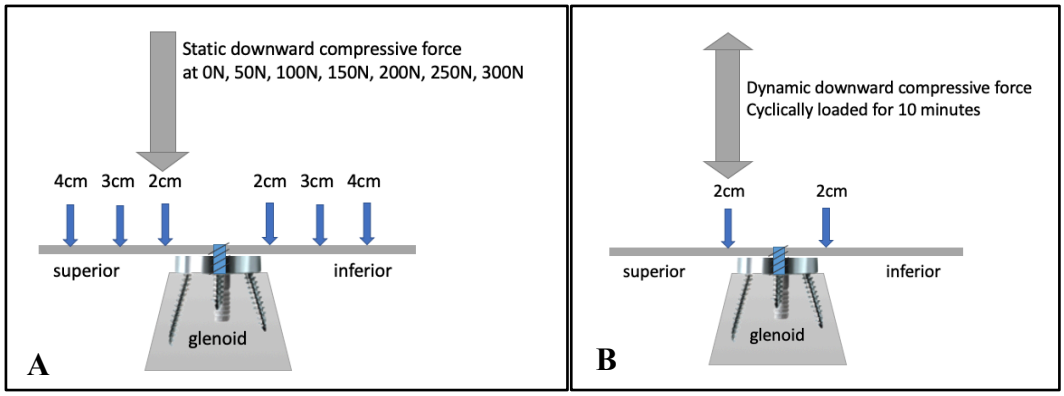

Figure 2-3: Schematic representation of the test apparatus.
A: Static Test: a static downward, axial, compressive force was applied at 50 N increments from 0N to 300N at 2cm, 3cm, and 4cm away from the glenoid baseplate center along an anatomical glenoid supero-inferior axis on the square plate (a total of six locations). The rigid plate was fixed to the glenoid baseplate via a central screw not extending into glenoid bone. B: Cyclic Test: a dynamic downward, axial, compressive force was applied cyclically for 600 cycles at a loading frequency of 1 Hz 2cm superiorly from the glenoid baseplate edge.
N = Newton. cm = centimeters. The large arrows at the top represent the actuator applying the downward static (A) and sinusoidal cyclic (B) force.

The test apparatus was aligned such that an axial downward force was applied perpendicular to the glenoid plane along the supero-inferior axis of the glenoid. The axial force is intended to simulate the net compressive external forces as well as active and passive soft tissue forces on the baseplate implanted into the glenoid in RTSA. This study employed two different testing protocols, static and cyclic loading. The static testing protocol (Figure 2-3 A) involved applying a downward, axial force onto the rigid plate-baseplate construct via an actuator statically for 30 seconds in each position, 2cm, 3cm, and 4cm superiorly as well as inferiorly from the glenoid edge, referred to as eccentric loading. Displacement measurements were taken before (at 0N) as well as at the end of applying each static compressive force to reveal the difference in displacement between the two. Thus, micromotion for the static protocol was defined as the difference in resting position of the implant before and after loading. The testing was non-destructive, and loading started at 0N at 50N increments and was terminated after the maximum load of 300N was achieved at each position. The cyclic testing protocol (Figure 2-3 B) consisted of applying a sinusoidal downward, axial, force of 300 N for 600 cycles at a loading

frequency of 1 Hz. Micromotion for the cyclic protocol was defined as the difference in peak motion between cycles.

Typical bending moments applied in the supero-inferior axis measured in-vivo in patients after total shoulder arthroplasty have been reported to be between 0-1.3 %BW*m[76] during activities of daily living. Assuming a patient mass of 75kg, the loading protocol outlined above covers a range of 0.15-1.6 %BW*m, with the purpose of investigating behavior in both regular and extreme conditions.

2.2.4 Statistical Analysis

Differences between groups in glenoid baseplate micromotion during static and cyclic loading were analyzed using multivariate analysis of variance (ANOVA). Reported p-values were two-tailed, and the minimum level of significance was assigned at $p<.05$. Statistical analyses were completed using IBM SPSS Statistics, version 26 (IBM, Armonk, NY, USA).

A post-hoc power analysis on an ANOVA, repeated measures and within factors, was performed to determine the actual power achieved, given the results (with alpha equals .05).

2.3 Results

During static testing, the average micromotion was not significantly different between the two screw configurations (Figure 2-4 A). The SI-locking group (n=10) had an average micromotion of 2.9±0.8μm and the AP-locking group (n=10) demonstrated 3.5±1.5μm of micromotion (p=.60). With regard to screw orientation (n=10 each), the baseplates containing parallel screws contained an average micromotion of 4.0±1.5μm and the result was not significantly different from the divergent screw orientation group, with an average micromotion of 2.0±0.7μm (p=.20). Within each sub-group (n=5) of screw configuration and orientation patterns, the average micromotion was as follows: SI-locking$_{divergent}$ = 1.9±0.2μm; AP-locking$_{divergent}$ = 2.6±1.5μm; SI-locking$_{parallel}$ = 4.6±1.4μm; and AP-locking$_{parallel}$ = 3.7±3.2μm (p=.595) and is shown in Figure 2-4 A.

Cyclic testing resulted in an average micromotion in the SI-locking group of 0.7±0.3µm and in the AP-locking group of 4.6±1.8µm (p=.08) (Figure 2-4 B). The parallel screw orientation group showed an average micromotion of 3.6±1.5µm and the divergent group had 1.7±0.6µm (p=0.402). The subgroups of n=5 each that were tested under cyclic conditions, demonstrated the following baseplate micromotions: SI-locking$_{divergent}$ = 0.8±1.4µm; AP-locking$_{divergent}$ = 2.6±3.1µm; SI-locking$_{parallel}$ = 0.6±0.6µm and AP-locking$_{parallel}$= 6.6±7.2µm. These were not significantly different from one another (p=0.215) and are represented in Figure 2-4 B.

A post-hoc power analysis revealed a power level of 99% between subject groups (N=5).

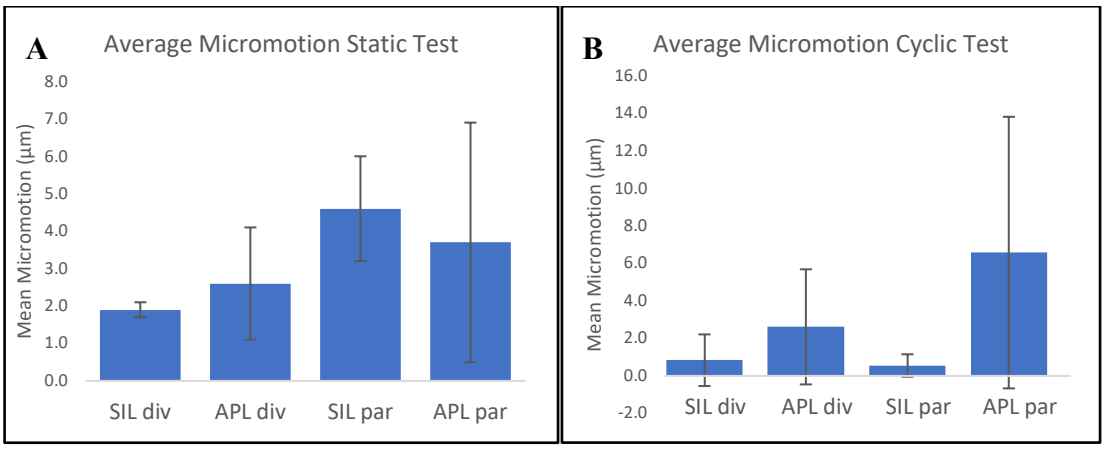

Figure 2-4: Average micromotion of the four subgroups by testing method.
A: Static testing revealed no significant difference between the four groups (p=0.595). B: Cyclic testing revealed no significant difference between the four groups (p=0.215). SIL div = supero-inferior locking divergent, APL div = antero-posterior locking divergent, SIL par = supero-inferior locking parallel, APL par = antero-posterior locking parallel.

After testing completion and removal of peripheral screws, manual manipulation of all baseplates via a simple 'wiggle test' revealed a macroscopically loose baseplate in one specimen from the AP- locking$_{parallel}$ group. This high degree of loosening after testing was also evident throughout testing, as the specimen demonstrated up to 50-times higher micromotion compared to the rest of the specimens (specimen 4 in Figure 2-5 A). This

specimen originated from a 70-year old male, whose cause of death was documented as amyotrophic lateral sclerosis (ALS) and, moreover, the corresponding contralateral shoulder specimen demonstrated high micromotion throughout testing (specimen 4 in Figure 2-5 B).

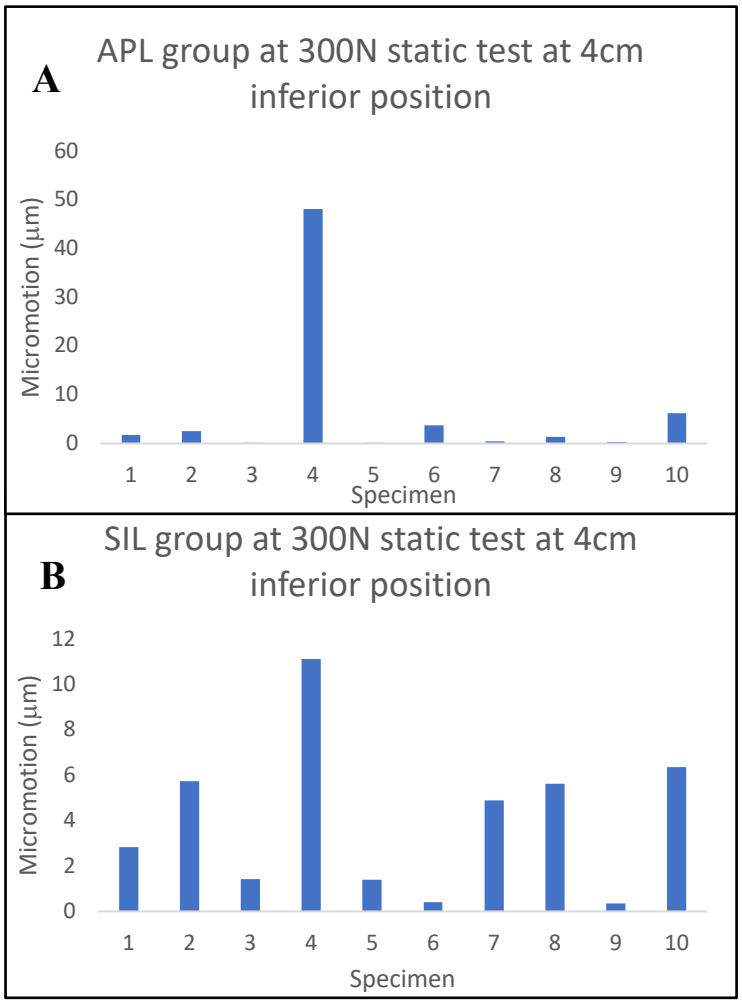

Figure 2-5: Micromotion between two different screw patterns, SIL and APL. *Each specimen number in A and B corresponds to one shoulder pair, left or right. SIL = supero-inferior locking, APL = antero-posterior locking, N = Newton, cm = centimeter*

2.4 Discussion

A long-standing practice in orthopedic surgery has been the use of hybrid screw fixation where a combination of locking and compression screws are used jointly. This concept

has been successful in locked plate osteosynthesis and has demonstrated advantage in providing the benefits of compression and fixation in the treatment of fractures[61–64]. Subsequently, authors have determined the applicability of hybrid screw fixation in reverse total shoulder arthroplasty baseplates, concluding that this method achieves secure glenoid baseplate fixation by maintaining micromotion below the necessary threshold of 150μm for bony ingrowth[65]. This study tested whether there is a difference in baseplate micromotion when the standard screw positioning is rearranged from the usual supero-inferior locking screw position to an antero-posterior locking screw position (thus, placing compression screws in the supero-inferior screw holes). The rationale behind choosing an antero-posterior locking construct was based on three reasons: (1) AP-locking is considered off-label usage as per the Food and Drug Administration, (2) AP-locking configuration has been used in several peer reviewed clinical outcome papers[77–80], and (3) there is little to no biomechanical literature to support or refute the usage of the AP-locking screw configuration.

In addition to considerations of screw position, previous authors have shown that a divergent screw orientation demonstrated less motion at the glenoid-baseplate interface compared to a parallel screw orientation[74]. Therefore, screw orientation (parallel versus divergent) was a secondary factor included in our analysis with the final aim to assist in best practice for surgical decision-making during RTSA procedures.

The overall outcome of this cadaveric biomechanical study indicates that screw position did not have a statistically significant effect on glenoid baseplate micromotion in the early, post-operative, fixation period. Additionally, we found that screw divergence bore no statistically significant difference in micromotion compared to parallel screw orientation, a finding shared in other biomechanical studies[68]. Though the AP-locking$_{parallel}$ group demonstrated a 2.5- to 11-fold larger micromotion than the remaining groups during cyclic testing, which was consistent with our initial hypothesis, the differences between either group were non-significant ($p=.215$). Considering that our study was sufficiently powered to evaluate whether there was a statistical difference or not, these results may be best explained by the average age and possibly better bone quality of our study population.

After testing completion and removal of peripheral screws, manual manipulation of all baseplates via a simple 'wiggle test' revealed a macroscopically loose baseplate in one specimen from the AP-locking$_{parallel}$ group. This high degree of loosening after testing was also evident throughout testing, as the specimen demonstrated up to 50-times higher micromotion compared to the rest of the specimens. This specimen originated from a 70-year old male, whose cause of death was documented as amyotrophic lateral sclerosis (ALS) and, moreover, the corresponding contralateral shoulder specimen demonstrated high micromotion throughout testing.

Overall, all scenarios, including locking screw position as well as the orientation of screw purchase, demonstrated micromotion well below the threshold for bony ingrowth. These results lend evidence to the conclusion made by previous authors that aiming peripheral screws into the best quality bone possible is a valuable consideration[49]. In addition, the average magnitudes of baseplate micromotion observed in this study are below the values cited in similar studies[68,81,82]. This can be attributed to not testing to failure or possibly due to variations in bone density in the cadavers tested. When interpreting the findings, we would like to emphasize that the use of cadaveric shoulders is a strength of the study as it provides more anatomic and material complexity than saw bone blocks. In addition, we have a large sample size for a cadaveric study n=20 and the study contains sufficient power to make statistically significant inferences about our results. Nevertheless, we advise to consider the following limitations. The shoulder specimens used in this study are exclusively male with an average age of 64±7 years and are, therefore, notably younger and may contain better bone quality than the average patient receiving RTSA surgery. Male gender is likely to be associated with higher bone density, and our results may be difficult to extrapolate to the female population. Overall, this indicates that the non-osteoporotic quality of this study's specimens may have led to a floor effect of data, because some RTSA patients may be more osteoporotic (patients with massive rotator cuff tears and proximal humerus fractures). Also, since this study was designed to compare the variables of screw insertion, we believe that the relative comparison amongst these variables would likely be similar with differing bone qualities, although the absolute magnitudes of displacement may change with more osteoporotic bone.

Another limitation is that this study focuses on circular baseplates only, emphasizing that the function of peripheral screw fixation is different in other commercially available baseplates. Lastly, this study focused on forces in the supero-inferior direction on the baseplate referred to as rocking-horse phenomenon, and it is important to note that there are additional forces impacting the baseplate during activities of daily living, such as shear forces, which were not studied. However, shear forces are accepted by the buttress between the screw and implant and given that the screws were well-fixed, it is likely that there would not be a difference in the supero-inferior or antero-posterior micromotion arising due to shear.

In addition, our results revealed large variability within the data. While the majority of specimens possess similar results in micromotion, some select specimens showed larger increases in baseplate micromotion. Since there was low irregularity in bone density among specimens seen in our study, it can be excluded as a potential cause for this finding. Moreover, no discernible pattern of applied load or position could be elicited that may explain the differences in micromotion among specimens. Lastly and more importantly, very low magnitudes of motion (micrometers) minimize the effect that differences between some of our results may have (i.e., large variations in micromotion between specimens and/or groups), thus, lending a potential explanation to their statistical insignificance.

Chapter 3

3 Type E2 Glenoid Bone Loss Orientation and Management with Augmented Implants

OVERVIEW

Glenoid erosion due to rotator cuff arthropathy represents a challenge during reverse shoulder arthroplasty and developing an understanding of the orientation and dimension of erosion is crucial to surgical success.

In this chapter, a computer-tomography based anatomy imaging software is applied to quantify the erosion orientation of the E2 type glenoid. In addition, in light of the new pathoanatomic findings, fatty infiltration of the rotator cuff was classified and surgical management with augmented implants of the eroded glenoid was assessed[b,c].

b) A version of this work has been published: Abdic S, Knowles NK, Walch G, Johnson JA, Athwal GA. Type E2 Glenoid Bone Loss Orientation and Management with Augmented Implants. *Journal of Shoulder and Elbow Surgery 2020 Jan*.

c) A portion of this work was used in a medical undergraduate activity: Favard Type E2 Glenoid Erosion Orientation and Quantification. *Research Trimester 2019.* Abdic S.

3.1 Introduction

Glenoid pathoanatomic changes can occur after long-term muscular imbalance associated with chronic rotator cuff insufficiency. Some authors[14,33,34] have described the incidence of pathologic bone remodeling in the context of cuff tear arthropathy nearing 40%[34,83], but knowledge on true incidence and severity of glenoid pathoanatomic changes is limited. Frankle et al. reported among all acquired glenoid bone loss scenarios undergoing reverse shoulder arthroplasty (RTSA), superior glenoid erosion (termed E2 by Favard et al.[37]) was the second most common erosion pattern, after the type B2[34]. The E2 erosion is caused by chronic superior migration of the humeral head due to a lack of constraint normally provided by the compressive forces of an intact rotator cuff.

Glenoid erosion due to rotator cuff arthropathy represents a challenge during reverse shoulder arthroplasty. Incorrect positioning of the glenoid baseplate due to deficient superior bone can result in residual superior tilt of the components. Superior tilt of the baseplate has been associated with an increased risk of aseptic loosening and instability[46,47]. Surgical techniques to address superior glenoid erosion in RTSA include asymmetric reaming, bone grafting, or the use of superiorly augmented baseplates[69].

The current literature suggests that E2 glenoid bone erosions are oriented purely superiorly as seen on standard anteroposterior radiographs or coronal Computed Tomography scans[38]. Roche et al. studied baseplate fixation for reverse shoulder arthroplasty in superiorly eroded E2 glenoids using composite scapulae (Pacific Research Laboratories, Vashon, WA, USA), in which they created a purely superior glenoid defect[82]. Our observational experience, viewing 3D CT scans and intraoperative assessments of E2 glenoids, has raised the question whether E2 glenoid erosions follow a predictable pattern different from purely superior. An understanding of the orientation of bone loss in a typical E2 glenoid has implications on baseplate fixation and rotational orientation of an augment. As such, the purposes of this study were two-fold. First, to quantify glenoid erosion and orientation from computed-tomography scans of patients with E2 glenoids. We hypothesized that the E2 erosion does not occur purely superiorly but is oriented in a predictable posterosuperior direction. Additionally, we hypothesized

that the degree of fatty infiltration within the rotator cuff would influence the orientation of the E2 erosion. The second purpose of this study was to examine four commercially available reverse baseplate designs used for the management of E2 erosions (standard, half-wedge, full-wedge, and patient-matched/BIO-RSA) with regards to the amount of bone volume removal necessary for proper seating.

3.2 Methodology

3.2.1 Patients

Clinical computed tomography (CT) scans (120-140 kVp, 512 x 512 resolution) were obtained from 40 patients with rotator cuff arthropathy containing type E2 glenoids (28 female and 12 male) at a mean age of 74 years (range, 56–88 years). The type E2 glenoids were classified according to Favard et al. as any glenoid with erosion limited to the superior aspect and not extending as far as the inferior glenoid rim[37,38]. All CT scans represented the most recently available pre-operative imaging of the shoulder pathology and were verified by two experienced shoulder surgeons.

3.2.2 Model Creation

Each CT scan was uploaded as a digital imaging and communications in medicine (DICOM) file to a medical imaging software program (Mimics v. 16.0; Materialise, Leuven, Belgium). Through standard segmentation techniques validated by Bryce et al.[84], the humerus and clavicle were manually separated from the scapulae to better visualise their glenoid. All segmentation was performed by the same investigator (S.A.), trained in the use of this medical imaging software program. Subsequent to segmentation, three-dimensional (3D) reconstructions were created as stereolithography files of each patient's scapula to reveal their morphological glenoid erosion (Figure 3-1).

Figure 3-1: 3D sagittal view of a right type E2 glenoid
An E2 type eroded glenoid with a postero-superiorly oriented erosion and a curved line-of-erosion (small black arrows) separating the neoglenoid (NG) from the paleoglenoid (PG).

Scapular anatomic reference planes were created by a modified method as described by Frankle et al[34] to allow for consistent referencing between scapular models. A scapular plane was created using three anatomically identifiable points on the scapula: the center of the glenoid, the trigonum spinae, and the inferior angle. Perpendicular to this scapular plane and through the centre of the glenoid, the sagittal plane was created to allow computational measurements[34].

3.2.3 Measurement of the Glenoid Surface Coordinate System

The anatomical landmarks of the supraglenoid and infraglenoid tubercles guided the creation of the supero-inferior (SI) axis[85] of the glenoid coordinate system (Figure 3-3 A), against which the orientation of glenoid erosion was measured in later steps. The perpendicular bisector of this SI-axis resulted in the antero-posterior (AP) axis of the glenoid, yielding the center of the glenoid and simultaneously dividing the glenoid in four quadrants: supero-anterior, supero-posterior, infero-anterior and infero-posterior (not

shown). Care was taken to correctly place the initial coordinate system as it would lay the foundation for further measurements and would give a basic orientation on the glenoid surface.

3.2.4 Measurement of the Angle of Orientation of the Erosion

The ridge of bone separating the paleoglenoid (original glenoid articular surface) from the eroded neoglenoid (newly eroded facet of the glenoid) was termed the line-of-erosion (Figure 3-1). All 40 of the 3D scapular models demonstrated a clearly defined curved line-of-erosion.

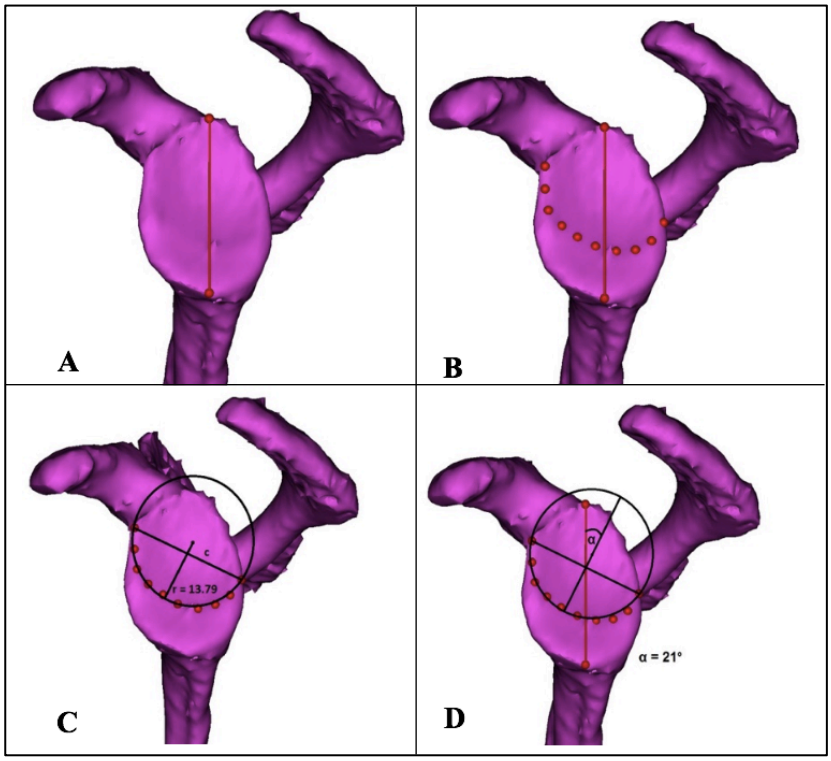

Figure 3-2: Obtaining the angle of erosion in a 3-D reconstructed model in a left shoulder.
A: The supero-inferior axis of the glenoid determined by the supra- and infraglenoid tubercles is drawn. B: Placement of ten coordinate points along the circular line of erosion results in a circle of best fit (C). Extending the radius (r) of the circle of best fit in a direction orthogonal to the chord (c), reveals the angle of erosion (α), as measured between the supero-inferior axis and the radius extension (D).
(S. Abdic, 2018)

This line of erosion was marked manually by placing ten 3D point coordinates along its course (Figure 3-2 B). This step allowed for the creation of a circle of best fit with its circle centre around the curved line of erosion (Figure 3-2 C). The two outermost points on the line of erosion, when connected, yielded the chord (c) of the circle. The radius (r) of the circle was placed orthogonally against the chord and when extended, resulted in the direction of the orientation vector (v) of erosion (Figure 3-2 D). Ultimately, the angle (α) between this vector and the previously established SI-axis resolved the erosion orientation angle. Thus, the vector of erosion indicates the overall erosion orientation, and is described by its angle (α) from the SI-axis.

To assess the extent of curvature of the line of erosion, the length of the radius of the circle of best fit was calculated. A larger circle of best fit (with a corresponding larger radius) results from a set of coordinate points placed along a less curved (flatter) line of erosion. In contrast, a smaller circle of best fit (with a corresponding smaller radius) results from a more circular line of erosion (see schematic representation in Figure 3-6). Accordingly, quantifying the magnitude of the radius gives us information about the extent of curvature of the erosion line.

The computation of the aforementioned steps was facilitated by a custom code developed in Matlab (MathWorks, Natick, MA, USA). The 3D point coordinates, the glenoid coordinate system, and the scapular and sagittal planes were extracted from mimics by the built-in medCAD module.

3.2.5 Surface Area of Erosion

To quantify the amount of erosion present in each patient's glenoid in this study, the reconstructed 3D scapulae were exported from Mimics into 3-matic (v. 8.0; Materialise)[86] along with the ten point coordinates along the erosion line. The articular surfaces of the neoglenoid (the eroded facet) and paleoglenoid (the remaining facet of the original glenoid surface) were marked by the built-in surface marking tools. Areas of calcified labrum and possible osteophytes were avoided in the highlighting procedure. This allowed for automated calculation of the surface area of the selected regions on the glenoid articular surface. The surface area of the neoglenoid facet was computed as a

percentage of the entire glenoid area (neoglenoid + paleoglenoid). To allow for further comparison and statistical analysis, severity of neoglenoid erosion was arbitrarily categorized into three sub-groups consisting of mild (0% to 33%), moderate (34% to 66%), and severe erosion area (>66%).

3.2.6 Fatty Infiltration of the Rotator Cuff

The severity of fatty infiltration of the rotator cuff muscles (supraspinatus, infraspinatus, subscapularis and teres minor) was assessed and classified according to Goutallier et al[87] as Grade 0 (no fat), Grade 1 (fatty streaks), Grade 2 (more muscle than fat), Grade 3 (equal muscle and fat), and Grade 4 (more fat than muscle)[87]. Fatty infiltration was visible by areas of decreased radiodensity using non-contrast CT scans in the sagittal oblique view ("Y-view") and was assessed by a senior shoulder surgeon as was previously described and validated[88–90].

3.2.7 E2 Reconstruction with Augmented Implants

The CT scans of a subgroup of 30 patients with E2 erosions were exported in DICOM file format to allow for further processing in a pre-operative planning software program (Glenosys®, ImascapTM, Brest, France). This software (Figure 3-3 A) automatically creates 3D reconstructions of the patient's scapula, allowing for simulated implantation of various glenoid augmentation designs (Figure 3-3 B-E).

The pre-operative planning program allows the implantation of various reverse baseplate designs within specified parameters. All baseplates tested were circular and either 25 or 29mm in diameter. The selection of the diameter of the baseplate and the glenosphere size (36, 39, 42mm) was made by an experienced shoulder surgeon. Once baseplate diameter and glenosphere size were selected for an individual patient, the same constructs were used for all scenarios with only the backside geometry of the implant varying. Four different backside baseplate designs were tested; standard, half-wedge, full-wedge and patient-matched (Figure 3-3 B-E). The standard baseplate was circular and flat backed. The half-wedge baseplate was circular and contained a half-wedge that was slanted at 35 degrees. The full-wedge baseplate was circular and contained a full wedge that was

slanted at 15 degrees. The patient-matched baseplate was circular with the backside geometry of the baseplate matching the patient's anatomy. The patient-matched baseplate design could also be used to represent a bony increased offset reverse shoulder arthroplasty (BIO-RSA), as the patient-matched metal portion can also represent a patient-matched bonegraft[91].

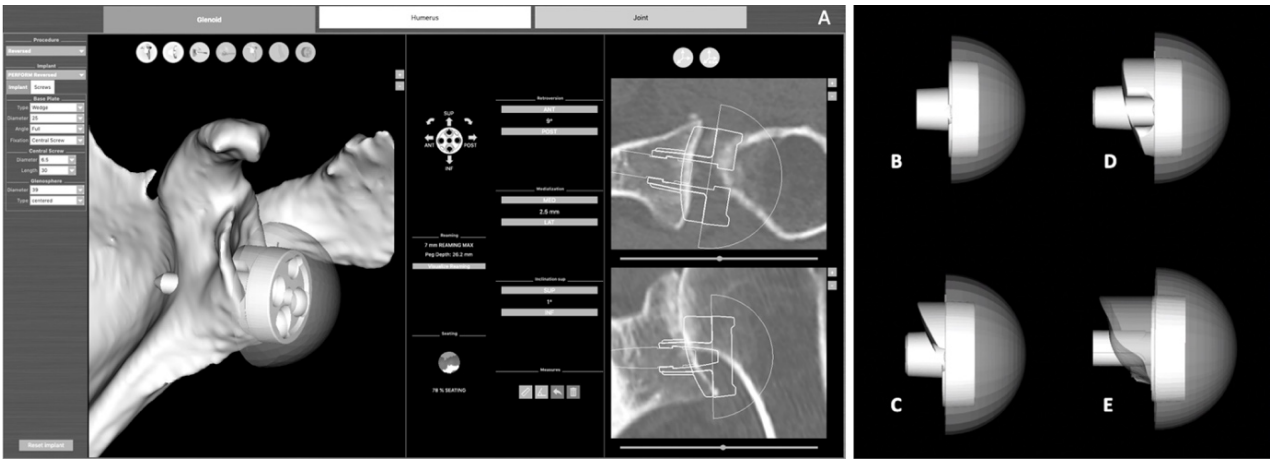

Figure 3-3: Surgical Planning Software and Augmented Baseplate Designs.
A screenshot view of the surgical planning software (A) used to implant a standard baseplate (B), a half-wedge augment (C), a full-wedge augment (D) and a patient-matched glenoid baseplate (E). The patient-matched baseplate was used to represent a patient-specific 3D printed implant or a Bony Increased Offset Reverse Shoulder Arthroplasty (BIO-RSA) design.

All baseplates were implanted by the same experienced shoulder surgeon within predetermined parameters: 0 to 10° of retroversion, 0° superior tilt, and >80% backside seating on host glenoid bone. Each case (30) was assessed without an implant and with all 4 baseplate implantations, for a total of 150 models. For each model, the volume of glenoid bone removal required for >80% seating was determined by recording the volume of the scapular model ('scapula bone mask') and the planned glenoid implant ('implant mask') as a volumetric 3D binary image. Retrieving the common voxels between the 'scapula bone mask' and the 'implant mask' through voxel-by-voxel comparison yielded the final bone removal to be measured. Additional software outcome parameters, such as lateralization and bony impingement-free range of motion

(adduction, abduction, flexion, extension, internal and external rotation) were recorded and compared between baseplate models.

3.2.8 Statistical Analysis

Demographic data and quantitative measures pertaining to erosion orientation in terms of angle and radii of curvature, surface area of erosion and severity were reported as means and standard deviations (SDs) for all 40 cases. Differences were evaluated using unpaired two-sided t-tests ($p<0.05$). Linear regression analyses were performed for the following parameters: erosion orientation angle, severity of erosion, curvature of line-of-erosion, age, and gender. Range of motion comparisons were compared among baseplate types using a one-way analysis of variance (ANOVA).

3.3 Results

The 40 superiorly eroded type E2 glenoids that were studied included shoulders from 28 female (70%) and 12 male (30%) patients at a mean age of 74 years (range, 56-88 years). The difference in age between genders was not statistically significant ($p=0.68$). Of the total, 27 (68%) were right and 13 (33%) were left shoulders.

3.3.1 Orientation and Angle of the Line of Erosion

The mean orientation angle between the vector of bony erosion and the supero-inferior axis of the glenoid was 47° ± 17° (range, 14° - 74°) located in the posterosuperior quadrant of the glenoid, resulting in the average erosion being directed between the 10 and 11 o'clock position on an imaginary clockface superimposed over the glenoid in a right shoulder (Figure 3-4).

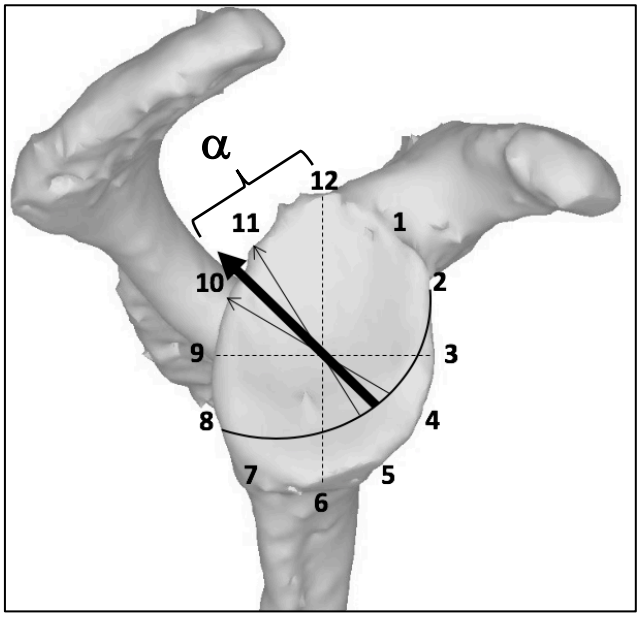

Figure 3-4: Mean orientation vector (± SD) of bony erosion in the entire cohort of E2 type glenoids.

(S. Abdic, 2018)

The mean E2 bony erosion orientation angle α (± SD) is located in the posterosuperior quadrant, measuring α = 47±17° from the supero-inferior axis (12 to 6 o'clock) of the glenoid. This results in the average erosion being directed at 10:30 on a right shoulder clockface.

glenoid coordinate system (supero-inferior and antero-posterior axis)

line of bony erosion

mean erosion vector orientation

standard deviation of erosion vector

The erosion orientation angle of the E2 bony erosion was not significantly different (p=0.38) between females (48±18°) and males (44±14°). When analyzing the orientation of the line of erosion by subgroup (mild, moderate and severe), a steady decrease in the angle of the erosion vector as severity of erosion increased was noted (Figure 3-5). In the one example of mild erosion in our cohort, the angle of the erosion vector was 70° away from the supero-inferior axis (no standard deviation calculable). The average erosion orientation angle in the moderate group was α = 51±15° and was not significantly different (p=0.37) from the severe group at α = 44±17° (Table 3-2).

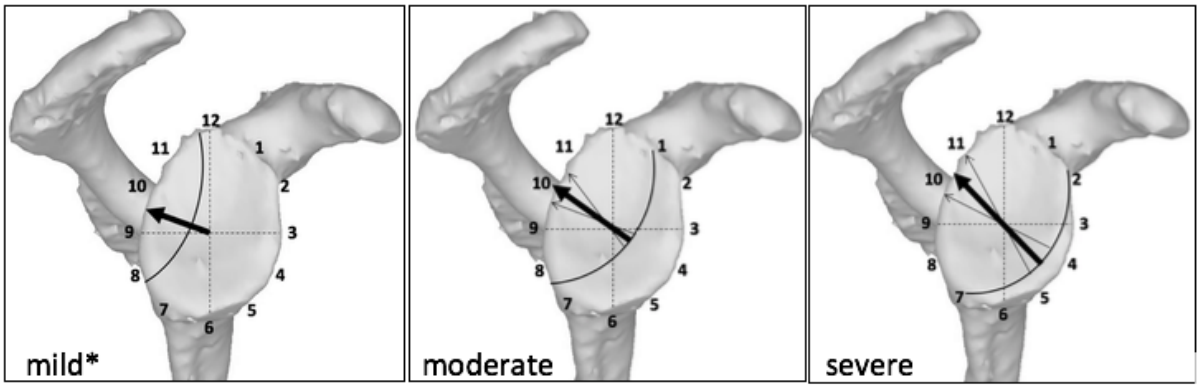

Figure 3-5: Mean orientation (± SD) of erosion in mild*, moderate and severe erosion.
There is a tendency of the erosion vector pointing progressively closer to 11 o'clock as erosion severity increases from mild to severe, but this tendency is not statistically significant (p=0.37). (S. Abdic, 2018)
** n=1. Standard deviation could not be calculated*

3.3.2 Surface Area

In the entire cohort, the mean surface area of the neoglenoid was 636 ± 247 mm^2 (range, 233 - 1,333 mm^2) and of the paleoglenoid 311 ± 165 mm^2 (range, 123 - 820 mm^2), revealing that, on average, the neoglenoids of the cohort consumed 67% of the total glenoid surface (average 946 ± 209 mm^2). The mean total surface area of the glenoid was 872 ± 169 mm^2 in women, and 1120 ± 194 mm^2 in men. In women, the mean surface area of the neoglenoid was 533 ± 191 mm^2, and in men 877 ± 190 mm^2; and the mean surface area of the paleoglenoid was 339 ± 170 mm^2 in women and 243 ± 137 mm^2 in men.

Expressing the neoglenoid erosion as a percentage of the total glenoid surface area resulted in three subgroups of erosion severity, containing 1 (3%) mild, 14 (5%) moderate, and 25 (63%) severe areas of erosion in the entire cohort. The corresponding surface area measurements according to gender are represented in Table 3-1 and according to subgroup in Table 3-2. Women and men differed significantly with regard to erosion severity ($p<0.001$). The eroded neoglenoids occupied 61% ± 17% of the total glenoid area in women, and 78% ± 11% in men, corresponding to a moderate and severe

erosion pattern, respectively. No correlation was found between severity of erosion and age, angle of erosion, or radius of erosion curvature.

Table 3-1: Demographic and anatomic features of male and female patients with E2 type glenoids erosions.

Measurement	Male (n=12)	Female (n=28)	p-value
Age (years)	73 ± 9 (56-85)	74 ± 7 (62-88)	0.68
Angle of erosion (°)	44 ± 14 (24-64)	48 ± 18 (14-74)	0.38
Radius of curvature (mm)	20 ± 5 (15-31)	22 ± 6 (13-36)	0.41
Area of Erosion (%)	78 ± 11 (severe)	61 ± 17 (moderate)	<0.001*

Values are mean ± standard deviation (range). P-values with a (*) indicate statistical significance.

Table 3-2: Demographic and anatomic features of mild, moderate, and severe type E2 glenoids with superior bone loss.

Measurement	All (n=40)	Mild (n=1)*	Moderate (n=14)	Severe (n=25)
Age (years)	74 ± 8 (56-88)	82*	72 ± 5 (63-78)	74 ± 9 (56-88)
Orientation angle of erosion (°)	47 ± 17 (14-74)	70*	49 ± 15 (16-67)	44 ± 17 (14-74)
Radius of curvature (u)	22 ± 6 (13-36)	26*	22 ± 6 (14-36)	21 ± 6 (13-32)
Area of Erosion (%)	78 ± 11	30*	48 ± 10 (34-63)	78 ± 6 (67-89)

Values are mean ± standard deviation (range). * n=1. Standard deviation and range could not be calculated.

3.3.3 Radius Measurements – Curvature of Erosion

For the entire cohort, the average radius of the circle of best fit around the curved line of erosion of the E2 glenoids was 22 ± 6 mm (range, 13-36 mm). The magnitude of the radius represents the extent of curvature of the line of erosion. A smaller radius belongs to a smaller circle of best fit, and thus, a more circular line of erosion on the glenoid (Figure 3-6). In contrast, a larger radius corresponds to a larger circle of best fit, representing a less curved (or flatter) line of erosion on the glenoid surface. The frequency of distribution of circle radii within the cohort of E2 glenoids is represented in Figure 3-6.

The positively skewed distribution of frequency graph of circle radii displayed in Figure 3-6 shows that the majority of the cohort contains glenoid erosion lines that are more hemispheric in shape. Accordingly, quantifying the magnitude of the radius gives us information about the extent of curvature of the erosion line.

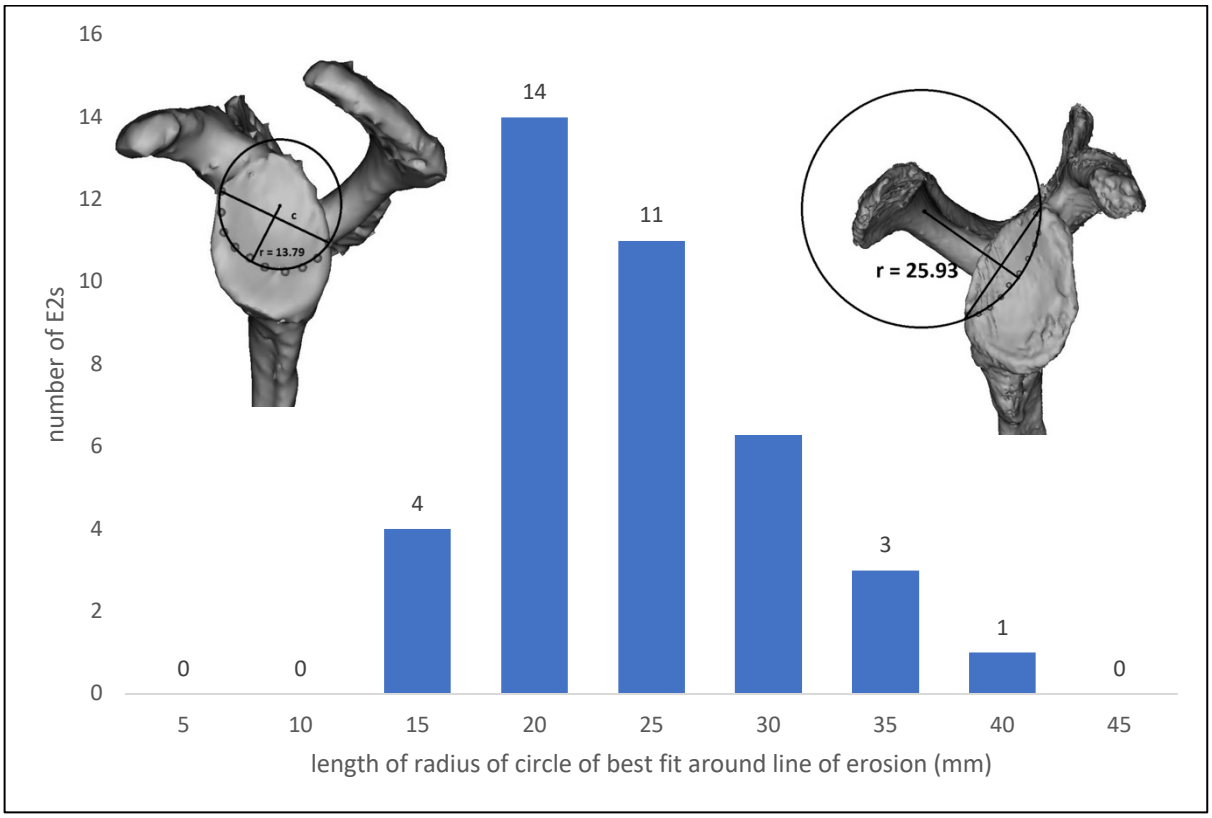

Figure 3-6: Distribution of radii of circles of best fit around the line of erosion in the entire cohort, measured in millimeters on the glenoid.
Top left shows a left shoulder with a largely circular/hemispheric line of erosion (dots) with a small circle of best fit and a corresponding small radius (solid line). Top right shows a less hemispheric/flat line of erosion in a right shoulder, with a larger circle of best fit and a larger radius.
(S. Abdic, 2018)

There was a low correlation between erosion curvature (radii) and erosion angles ($r = 0.45$), but the radius of erosion was not correlated with erosion area (severity of erosion). The difference between radii in females (22 ± 6 mm) and males (20 ± 5 mm) was not statistically significant ($p = 0.41$). Analyzing the difference in curvature by erosion

severity (mild, moderate, severe) revealed that mean radii appear to have a continuously decreasing trend within each subgroup, but the difference in mean radii between moderate and severe erosion was not statistically significant (p=0.718). The mean radius in the one mild subject was 26 mm (no standard deviation calculable). In the 14 moderate subjects it was 22 ± 6 mmm, and in the 24 severe subjects it was 21 ± 6 mm (Table II).

3.3.4 Virtual Implantation and Bone Volume Removed

In the 30 subjects that were used to virtually implant four different baseplate designs, the average volume of glenoid bone removed was lowest for the patient matched design (mean, 200 ± 297 mm^3, range 0 – 995 mm^3) and highest for the standard (no augment) design (mean, 4009 ± 1210 mm^3, range 1954 – 6915 mm^3). The full wedge design (1228 ± 753 mm^3, range 354 – 3742 mm^3) removed less bone volume than the half wedge design (1763 ± 969 mm^3, range 597 – 4290 mm^3). The differences between each scenario were statistically significant and are depicted in Figure 3-7. There was no significant difference in bone volume removal by gender in any of the four baseplate scenarios ($p > .05$).

After implantation in Glenosys®, the average virtual implant data in terms of glenosphere and baseplate diameter, pre- and post-operative glenoid version and glenoid depth measurements including final range of motion measurements for each baseplate design are listed in Table 3-3 for comparison.

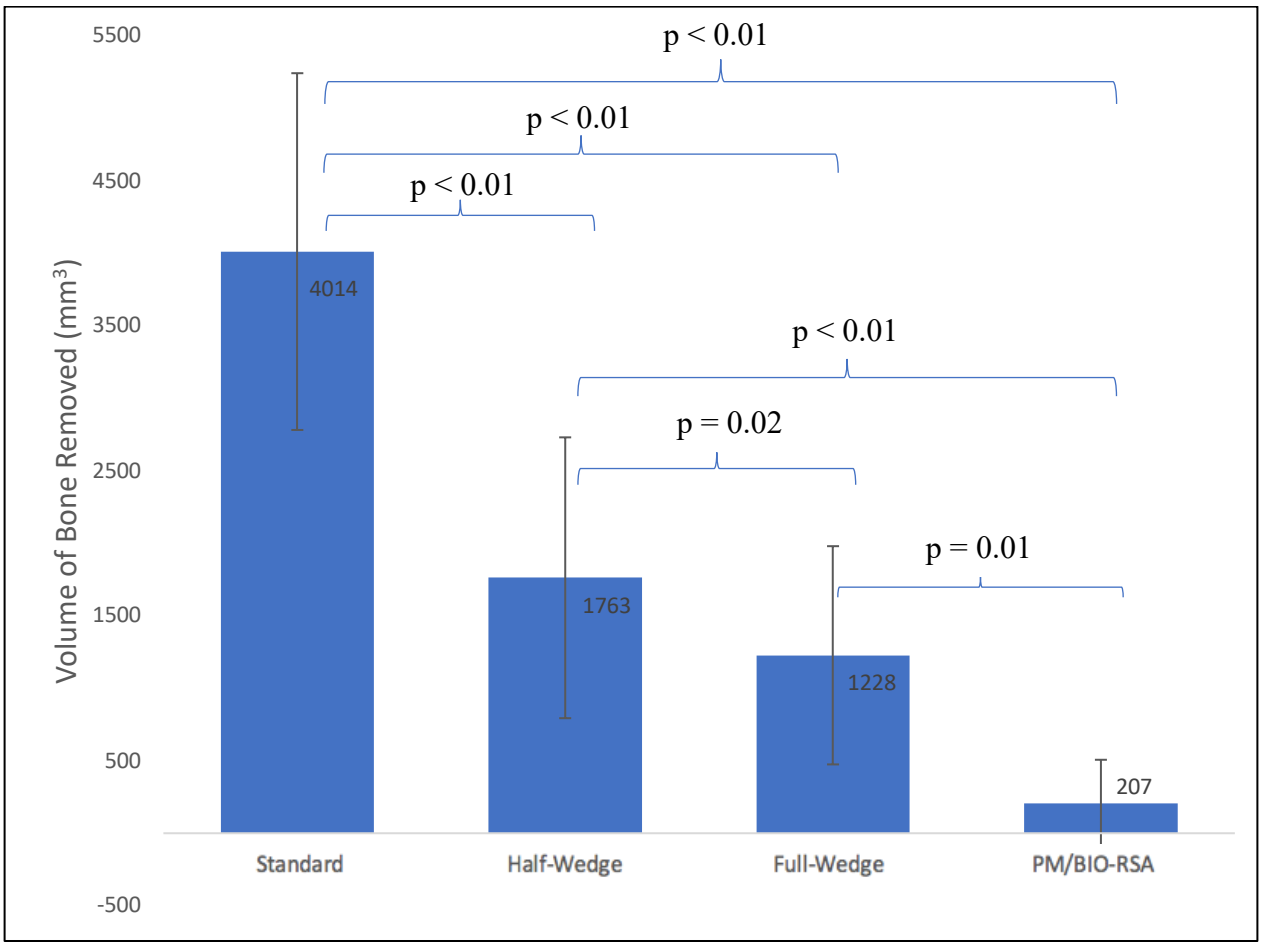

Figure 3-7: Average Glenoid Bone Removal
Average glenoid bone volume removed for minimum 80% backside seating of four different baseplate designs placed at an average 10° retroversion: patient matched, full wedge, half wedge, no augment.
Differences in average bone volume removed between each augment design reached statistical significance (p<.05).

Analyzing the difference between volume of bone removed between moderate and severe erosion revealed that in all four scenarios, more bone volume was removed in the severe erosion pattern. There was no statistical difference in volume of bone removed between moderate and severe erosion patterns in any of the four baseplate augment designs (p >0.05).

Table 3-3: Virtual implant design parameters and post implantation outcome measures for all four baseplate augmentation scenarios.

Implant Data	*Baseplate Diameter (mm)*		*Glenosphere Diameter (mm)*		
All (n=30)	25 (n=21)	29 (n=9)	36 (n=11)	39 (n=12)	42 (n=7)
Measurements	*Glenoid Version (mean °)*		***Final State***		
	pre-op	post-op	*Global Lateralization (mm)*		
Standard	12 retroversion	8 retroversion	2		
Half-Wedge	12 retroversion	8 retroversion	5		
Full-Wedge	12 retroversion	9 retroversion	9		
Patient-Matched	12 retroversion	9 retroversion	10		
Impingement-Free Range of Motion	*Add. (°)*	*Abd. (°)*	*Ext. (°)*	*Flex. (°)*	*Int. Rot. (°)*	*Ext. Rot.(°)*
Standard	8*	78	32*	85*	66	22*
Half-Wedge	16*	81	52*	114*	77	41*
Full-Wedge	24*	84	80*	125*	79	53*
Patient-Matched	25*	85	88*	125*	79	56*

Add. = adduction, Abd. = abduction, Ext. = extension, Flex. = flexion, Int. Rot. = internal rotation, Ext. Rot. = external rotation
(*) indicates significant difference between baseplate designs ($p<0.05$)

3.3.5 Fatty Infiltration of the Rotator Cuff

Among the 40 subjects with E2 glenoid deformities, 35 (88%) had a Goutallier grade 4 fatty infiltration of the supraspinatus (SSP) and 31 (78%) had a Goutallier grade 4 fatty infiltration of the infraspinatus (ISP). The distribution of occurrences within the cohort by grade of fatty infiltration within each rotator cuff muscle is shown in Table 3-4. Within the subscapularis (SSC) muscle, the majority of subjects (n= 18, that is 45%) showed a grade 1 fatty infiltration, whereby 4 (10%) had a grade 4 fatty infiltration. The teres minor (TM) muscle contained mostly grade 1 fatty infiltration (n= 13, that is 33%). No subjects showed a fatty infiltration of the SSP or ISP lower than grade 2.

Table 3-4: Goutallier Grades of Fatty Infiltration of Individual Rotator Cuff Muscles in the Series.

	Grade 0	Grade 1	Grade 2	Grade 3	Grade 4
Supraspinatus	-	-	1	4	35
Infraspinatus	-	-	5	4	31
Subscapularis	1	18	10	7	4
Teres Minor	1	13	10	5	4

Values are total number of cases 'n'.

The largest of the rotator cuff muscles, the subscapularis, exhibited a grade 0 fatty infiltration in one subject (2.5%), grade 1 in 18 (45%) subjects, grade 2 in 10 (25%), grade 3 in 7 (17.5%), and grade 4 in 4 (10%) subjects overall. Comparing the effect its fatty infiltration may have on erosion orientation and erosion line radii in the entire cohort revealed large variability overall. A noticeable difference in the angles of erosion from grade 3 subscapularis fatty infiltration to grade 4 subscapularis fatty infiltration may be observed in Figure 3-8. Grade 3 fatty infiltration of the subscapularis muscle is implicated in erosion vectors pointing towards the 9:30 or 10 o'clock direction, whereas Grade 4 fatty infiltration of the subscapularis is implicated in the erosion vector pointing towards 11:30 on the glenoid clockface.

The seven subjects exhibiting Grade 3 fatty infiltration of the subscapularis muscle are clustered in a higher range of erosion angles (between 50° - 72°), while the four subjects with Grade 4 subscapularis fatty infiltration were clustered in the lower region of erosion angles (between 16° and 29°). The mean angle of erosion by grade of subscapularis fatty infiltration is presented in Table 3-5.

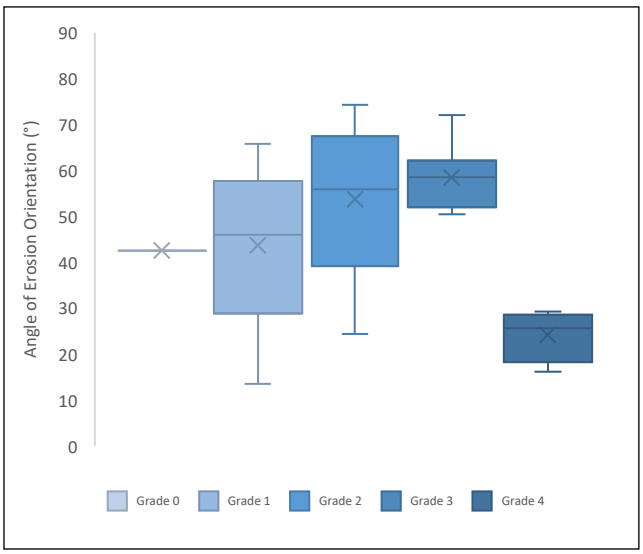

Figure 3-8: Subscapularis Fatty Infiltration Grade versus Erosion Orientation Angle (°).
There was a statistically significant decrease ($p<0.001$) in the erosion orientation angle between patients with grade 4 fatty infiltration of the subscapularis versus lower grades.

The difference in mean angles of erosion between Grade 4 fatty infiltration of the subscapularis and lower grades was statistically significant ($p<0.001$).

Table 3-5: Mean angles of erosion (°) by grade of subscapularis muscle fatty infiltration

SSC grade of fatty infiltration	Subjects	Mean angle of erosion (°) ± SD	Glenoid clockface representation
Grade 0	1	43*	10:30
Grade 1	18	44 ± 16	10:30
Grade 2	10	54 ± 16	10:00
Grade 3	7	58 ± 7	10:00
Grade 4	4	24 ± 6	11:00

(*) no standard deviation calculable.

3.4 Discussion

Some degree of glenoid bone loss is a relatively common finding in reverse shoulder arthroplasty and failure to adequately address glenoid erosion in the context of baseplate fixation can lead to substandard outcomes [37,59,92]. Different operative methods aiming at adequate baseplate fixation during reverse shoulder arthroplasty in eroded glenoids have been described[54,69,82,93–95]. To date, there is lack of knowledge on true morphology and orientation of glenoid erosion in patients with rotator cuff arthropathy and chronically acquired glenoid defects. To consider the best and most viable treatment option in reverse shoulder arthroplasty, developing a fair understanding of the morphology, size and orientation of erosion in glenoid bone loss is imperative.

This present study has revealed that in patients with acquired superior glenoid bone loss of Favard type E2, the average orientation of erosion is directed between the 10 and 11 o'clock position, corresponding to the supero-posterior quadrant on the glenoid in a right shoulder. This is in agreement with this study's hypothesis that the neoglenoid in E2 eroded glenoids is not purely contained within the superior aspect of the glenoid surface. The average vector of orientation was at an angle of $\alpha = 47° \pm 17°$ (range, 14° - 74°) measured from the supero-inferior axis in the supero-posterior quadrant on the glenoid. Larger α angles correspond to an orientation further from the supero-inferior axis and are, thus, more posterior while smaller angles are closer to the supero-inferior axis and coincident to a more superior direction of orientation. All 40 cases of E2 erosions in this study were contained within the supero-posterior quadrant of the glenoid only. To further describe erosion characteristics, the surface area of the neoglenoid as a percent of the total glenoid area was determined. The neoglenoids of the cohort consumed, on average, 67% of the total glenoid surface, which was classified as severe erosion. The severity of erosion was termed mild, moderate or severe by arbitrarily dividing the cohort into three subgroups determined by the percent area of the neoglenoid versus total area of the glenoid (mild 0% to 33%, moderate 34% to 66%, and severe erosion area >66%). Though data based on this willful assignment may be used with discretion, one can certainly agree that an average erosion area of closely two thirds the original glenoid area is substantial. Given that baseplate fixation occurs in the inferior two-thirds of the glenoid,

a supero-posterior erosion of 67% of the total glenoid surface inevitably affects proper positioning and affixation of the baseplate. The orientation of the line of erosion was analyzed by subgroup (mild, moderate and severe), and we found that increasing erosion severity resulted in progressively more superiorly oriented erosion with further erosion of the paleoglenoid, though the change was not found to be statistically significant ($p=0.37$) and is likely due to the low number of specimens per sub-group.

As our understanding of the progression of glenoid bone loss over time[96] is in the beginning stages, these results are certainly interesting to acknowledge. Based on this data, it is likely that there may be a timely connection between E2 glenoids and E3 glenoids.

Surgeons managing patients with E2 type bone loss should be aware of the orientation of erosion facing the 10 and 11 o'clock position, as none of the subjects measured in this study exhibited a pure superior (12 o'clock) orientation of erosion. Additionally, a curved line of erosion was identified between the paleoglenoid and the neoglenoid in every E2 glenoid in this study, with a large proportion being very curved as evidenced by the positively skewed distribution graph of circle radii in Figure 15. How this hemispheric line of erosion develops and what factors may be involved in shaping a very curved versus less curved line of erosion is still unclear. In this study on B2 glenoid erosion and orientation, Knowles et al. noted a curved line of erosion in 19 out of 55 (35%) cases studied[85]. They theorized that the humeral head was related to these erosive patterns by eroding the glenoid via rotation rather than translation but were unable to find a discernible relationship between the two. This suggests that there may be multiple unknown factors involved in the morphology and orientation of bone loss in glenoid erosion.

The mean erosion orientation towards the supero-posterior quadrant, the mean severity of erosion area of two-thirds the glenoid area and the curved line of erosion in the 40 E2 glenoids measured in this study are all relevant considerations for the surgeon who is treating E2 type glenoid bone loss with augmented glenoid components. Martin et al. assessed the initial fixation stability in RSA glenosphere baseplates by varying the extent

of superior glenoid bone loss in bone foam models and found significantly reduced fixation when more than 50% of bone loss was present under the baseplate[97].

In the current study, a virtual simulation of the filling of the supero-posterior glenoid defect by varying the choice of augmented baseplates (full wedge, half wedge, standard and patient specific bone grafting) was undertaken. The augment scenario with least amount of bone volume removal was the patient specific bone grafting procedure. Correcting severe bone loss through high side reaming results in further bone loss and is best minimized or avoided, therefore, several authors assert bone grafting to be a good option to account for bone loss in glenoid erosion[33,94]. However, with the possibility of graft resorption or migration and contraindications, such as humeral head necrosis, the use of bone graft procedures in correcting glenoid bone loss becomes a difficult procedure even for the most experienced surgeon. Surgeons managing patients with E2 type glenoids considering bone grafting should be aware of the supero-posterior orientation of erosion. The orientation of erosion becomes more relevant when considering commercially available augments such as standard, full wedge or half wedge components. Among the three basic shapes of augment components in this study, the full wedge was found to be the most bone preserving augmentation option in both males and females with moderate as well as severe erosion patterns. Some authors have reported on glenoid erosion augmentation options in posteriorly eroded B2 glenoids and found the half wedge component to be the most bone preserving in this type of glenoid defect[98–100]. The results herein may differ from the literature due to the hemispheric nature of the erosion line present in every single case in this series. Commercially available wedged designs, even if oriented correctly towards the 10 or 11 o'clock position in E2 glenoids, contain a linear decline in their step whereas erosion in this study cohort was hemispheric and may, thus, be a better fit for the use of full wedge designed augmentation. Examining the virtual implant parameters both pre-operatively and post-operatively revealed the full wedge most closely approximating the patient specific bone augmentation design in terms of global lateralization, anteriorization, distalization and most importantly, range of motion after implantation. Though intuitively expected and as previously concluded by other authors [98–100], standard augmentation components are the least favorable option to

account for asymmetric glenoid bone loss when bone preservation is sought. Standard augmentation was also implicated in the lowest range of motion, as measured by the virtual implantation software in this study. Though no statistical difference in bone volume removed was found between moderate and severe erosion in all four augmentation scenarios, the amount of bone removed was consistently higher in the severe erosion group than in the moderate erosion. Thus, there may be benefit in early recognition of bony erosion in E2 type glenoids as delay in treatment may result in increased erosion severity and expanded bone volume removal for proper baseplate positioning. As expected, these results also show that volume of bone removed was highest among lower radii of erosion (more curved erosion lines) in both moderate and severe erosion subgroups. These results reveal that a straighter line of erosion produced less bone volume removal while a more curved line of erosion produced more bone volume removal during the positioning of the four baseplate scenarios. This may be related to different requirements for reaming when a curved line of erosion is present to adequately prepare the glenoid surface for proper seating of the baseplate. A straight erosion line may require less re-modelling to improve osseous contact with commercially available augments such as the half wedge design containing a straight-line step.

The participation of the rotator cuff's fatty infiltration in the development of glenoid morphology has recently begun to become a focus of study. Donohue et al. retrospectively studied different patterns of pathologic glenoid bone loss in conjunction with rotator cuff muscle fatty infiltration and found increased fatty infiltration in association with B3 glenoids and increased pathologic retroversion[101]. Walker et al. demonstrated differences in fatty infiltration of the posterior rotator cuff between A-type and B-type glenoids. In my study, the degree of fatty infiltration was severe (Grade 4) in the supraspinatus muscle in 35 cases (88%) and in the infraspinatus muscle in 31 cases (78%). This is consistent with the orientation of erosion towards the supero-posterior quadrant of the glenoid. These results, in agreement with the above-mentioned studies, support the notion that there may be a causal relationship between fatty infiltration of the rotator cuff muscles and glenoid morphology, but the clinical relevance of this is still unknown.

The post-operative state of fatty infiltration of the rotator cuff following RTSA may influence the centering of the prosthetic humeral head much like the pre-operative state of fatty infiltration may have been involved in creating distinct erosion patterns on the glenoid surface in the first place. To investigate this further, I looked at the degree of fatty infiltration of the subscapularis muscle and how it may affect erosion orientation. While the majority of the cases in this study demonstrated a mild subscapularis muscle fatty infiltration, I found a marked difference in erosion orientation as the grade of fatty infiltration of the subscapularis muscle increased from Grade 3 to Grade 4. Grade 3 fatty infiltration of the subscapularis muscle was implicated in erosion vectors pointing towards the 9:30 or 10 o'clock direction, whereas Grade 4 fatty infiltration of the subscapularis was implicated in the erosion vector pointing towards 11:30 on the glenoid clockface. A possible explanation for this change in erosion orientation towards a more superior direction may be the greater influence of the intact deltoid muscle, by superiorly pulling the humeral head with weaker subscapularis muscle involvement. This is certainly interesting to investigate further, as there may be a tendency of glenoid erosion to point superiorly and supero-anteriorly with increasing subscapularis fatty infiltration. None of my cases studied demonstrated a supero-anterior erosion and this is consistent with the overall low fatty infiltration of the subscapularis muscle throughout the cohort.

Certainly, there are limitations to this study. Severity of glenoid erosion was measured by the area of erosion divided by the total glenoid area as seen from an en-face view of the glenoid only. This process does not account for the slope of erosion, represented by the inclination of the neoglenoid, which certainly is a major contributing factor to the amount of bone loss actually present. Therefore, two glenoids with the same area of erosion may have very different amounts of bone loss present and this is not taken into account by our definition of severity of erosion.

Additionally, arbitrarily dividing surface area of erosion in three thirds represents a challenge for statistical analysis. Several values were close to the cut off value and though we only had one mild case (<33% of area eroded) in this series, 3 further cases came very close to it (34% and 35% of erosion). To further understand glenoid bone loss orientation, severity and its progression over time, we recommend a unified way of

assessing severity including both the area of erosion as well as the inclination of the neoglenoid.

Chapter 4

4 Summary and Conclusion

4.1 Summary of Chapter 2

This study assessed whether there is a difference in baseplate micromotion when the standard screw positioning is rearranged from the usual supero-inferior locking screw position to an antero-posterior locking screw position (thus, placing compression screws in the supero-inferior screw holes). The rationale behind choosing an antero-posterior locking construct was based on the following three reasons: (1) AP-locking is considered off-label usage as per the Food and Drug Administration, (2) AP-locking configuration has been used in several peer reviewed clinical outcome papers[77–80], and (3) there is little to no biomechanical literature to support or refute the usage of the AP-locking screw configuration.

In addition to screw position, screw orientation (parallel versus divergent) was a secondary factor included in the analysis.

This study revealed no statistically significant quantitative difference in baseplate micromotion between screw position or orientation in a circular reverse total shoulder arthroplasty baseplate in non-eroded glenoids. Additionally, the results demonstrated no significant differences between parallel and divergent screw orientation on baseplate micromotion.

Overall, these results corroborate that surgeon preference is central in the selection of screw position (locking screws AP versus SI) and orientation (parallel versus divergent).

4.2 Summary of Chapter 3

Correct alignment of glenoid components in RTSA is essential for full osseous contact with the glenoid, and above all, accurate surgical implantation of the baseplate is paramount when glenoid erosion is present. This study revealed that the average orientation of erosion in Favard's E2 glenoids is directed in the supero-posterior quadrant on the glenoid. Considering this orientation of glenoid bone loss, the full wedge baseplate design resulted in the least amount of bone volume removed for a minimum of 80% back-side seating. Of note, the study in this chapter unexpectedly revealed that the degree of subscapularis muscle fatty infiltration may have more influence in changing the orientation of erosion than previously thought.

Overall, this study serves as the basis for correct surgical planning of baseplate positioning in supero-posteriorly eroded E2 glenoids and elucidates correct baseplate orientation when considering a full-wedge augmented baseplate.

4.3 Thesis Conclusion

Improving glenoid baseplate fixation in reverse total shoulder arthroplasty continues to be a significant focus of research in an endeavor for improving overall patient outcomes and extending implant longevity. Glenoid fixation in the normal glenoid is well established in the literature, and this thesis adds an unknown contribution pertaining to peripheral screw fixation of a glenoid baseplate in the non-eroded glenoid. The results herein indicate that screw position did not have a statistically significant effect on glenoid baseplate micromotion in the early, post-operative, fixation period. Additionally, screw divergence bore no statistically significant difference in micromotion compared to parallel screw orientation, a finding shared in other biomechanical studies[68]. These results add to the conclusions made by previous authors that aiming peripheral screws into the best quality bone possible is a valuable consideration[49].

Additionally, the findings in this thesis add to advancement of research into the quantification of glenoid erosions including their best surgical management with regards to baseplate fixation in RTSA. With respect to the acquired erosion in a Favard E2 type glenoid, the findings herein revealed that the average orientation of erosion is directed within the supero-posterior quadrant on the glenoid and that, on average, 67% of the total glenoid surface is affected (classified as severe erosion). Given that baseplate fixation occurs in the inferior two-thirds of the glenoid, these findings inevitably affect proper positioning and affixation of the baseplate. Therefore, this thesis revealed that when using commercially available augmented baseplate components in supero-posteriorly eroded E2 glenoids, the full wedge baseplate is the most bone preserving augmentation option, provided it is oriented correctly in the supero-posterior direction on the glenoid. With this unconventional orientation of the baseplate away from the imagined supero-inferior and antero-posterior coordinate system on the glenoid and in conjunction with the findings of the previous study in Chapter 2, the overall summative conclusion of the thesis emphasizes that correct orientation of the baseplate takes precedence over appropriate coordinate axis (supero-inferior/antero-posterior) alignment. Surgeon preference in aiming for the best bone quality possible is preferred and evidence is provided herein that helps improve overall baseplate stability in RTSA.

To conclude, after analyzing the overall results, we propose the suggested baseplate orientation for the deficiency pattern seen in E2 type glenoids to be facing towards the erosion orientation in the postero-superior direction on the glenoid. In addition, previous authors have demonstrated that glenoid bone density is highest precisely below the erosion[102]. Thus, considering that the densest bone is the best quality of bone for the purpose of glenoid baseplate fixation in RTSA, it is presumably correct to extrapolate the results from the glenoid fixation study in Chapter 2 and to suggest that locking or non-locking screw position and orientation may not affect micromotion in the eroded glenoid. Therefore, the evidence presented in this thesis substantiates the notion that surgeons managing patients with E2 type glenoid erosion may orient peripheral baseplate screws towards the best quality bone possible. Additionally, it gives surgeons the option to give consideration to intrinsic mechanical factors of locking or non-locking screws when considering their position on the baseplate other than abiding by the recommended and most frequently used supero-inferior locking screw/ antero-posterior compression screw orientation.

4.4 Future Directions

The research findings in this thesis have implications for future clinical and biomechanical studies. The results in the above-mentioned investigations suggest that orienting the baseplate in a way that directs peripheral screws into the best quality bone possible, leads to satisfactory baseplate fixation in non-eroded glenoids during RTSA procedures. This result is due to the lack of statistically significant difference between the position and orientation of peripheral locking screws in a circular RTSA baseplate found in this thesis. To extrapolate what these results signify in eroded glenoids, this research quantified the orientation of erosion in an E2 type glenoid and, thus, demonstrated that accurate orientation of a full-wedge augmented baseplate towards the supero-posterior quadrant would lead to the least bone removal necessary as well as allow the surgeon to orient peripheral screws away from the standard imaginary coordinate system of the glenoid in order to facilitate best baseplate fixation.

The inquiry on the E2 type of glenoid erosion in light of accurate baseplate orientation and peripheral screw positioning lays the groundwork for further research into the quantification of glenoid erosions including their best surgical management with regards to baseplate fixation in RTSA. The cause of glenoid bone loss and its progression over time is still unclear, and thus, future investigations may build on assessing the influence that fatty infiltration, especially that of the subscapularis muscle, may have on the orientation of glenoid erosions.

5 References

1. Terrier A, Reist A, Vogel A, Farron A. Effect of supraspinatus deficiency on humerus translation and glenohumeral contact force during abduction. *Clin Biomech*. 2007. doi:10.1016/j.clinbiomech.2007.01.015

2. Culham E, Peat M. Functional anatomy of the shoulder complex. *J Orthop Sports Phys Ther*. 1993. doi:10.2519/jospt.1993.18.1.342

3. Culham E, Peat M. Functional anatomy of the shoulder complex. *J Orthop Sport Phys Ther*. 1993;18(1):342-350.

4. Neer II CS. Shoulder reconstruction. In: *Shoulder Reconstruction*. ; 1990:1-551. doi:10.1080/03115519808619195

5. Peat M. Functional anatomy of the shoulder complex. *Phys Ther*. 1986;66(12):1855-1865. doi:10.1093/ptj/66.12.1855

6. Saha AK. Dynamic stability of the glenohumeral joint. *Acta Orthop*. 1971;42(6):491-505. doi:10.3109/17453677108989066

7. Sarrafian SK. Gross and functional anatomy of the shoulder. *Clin Orthop Relat Res*. 1983;(173):11-19. doi:10.1097/00003086-198303000-00003

8. Rothman R, Marvel JJ, Heppenstall R. Anatomic considerations in the glenohumeral joint. *Orthop Clin North Am*. 1975;6(2):341-352.

9. Langohr GDG. Fundamentals of the Biomechanical Characteristics Related to the Loading of Reverse Total Shoulder Arthroplasty Implants and the Development of a Wear Simulation Strategy. 2015;(January).

10. Lee TQ. Clinical Anatomy and Biomechanics of the Glenohumeral Joint (Including Stabilizers). In: *Shoulder Instability : A Comprehensive Approach*. ; 2012:531.

11. Zingg PO, Jost B, Sukthankar A, Buhler M, Pfirrmann CWA, Gerber C. Clinical

and structural outcomes of nonoperative management of massive rotator cuff tears. *J Bone Jt Surg - Ser A*. 2007;89(9):1928-1934. doi:10.2106/JBJS.F.01073

12. Milgrom C, Schaffler M, Gilbert S, van Holsbeeck M. Rotator-cuff changes in asymptomatic adults. The effect of age, hand dominance and gender. *J Bone Joint Surg Br*. 1995;77-B(2):296-298. doi:10.1302/0301-620X.77B2.7706351

13. K.J. E, T.Q. L, J. T, R. G. Rotator cuff tear arthropathy. *J Am Acad Orthop Surg*. 2007;15(6):340-349. http://ovidsp.ovid.com/ovidweb.cgi?T=JS&PAGE=reference&D=emed8&NEWS=N&AN=17548883.

14. Neer CS, Craig E V., Fukuda H. Cuff-tear arthropathy. *J Bone Jt Surg - Ser A*. 1983;65(9):1232-1244. doi:10.2106/00004623-198365090-00003

15. Gumina S, Candela V. Rotator cuff arthropathy. what is it? In: *Rotator Cuff Tear: Pathogenesis, Evaluation and Treatment*. ; 2016:383-390. doi:10.1007/978-3-319-33355-7_46

16. Wening JD, Hollis RF, Hughes RE, Kuhn JE. Quantitative morphology of full thickness rotator cuff tears. *Clin Anat*. 2002;15(1):18-22. doi:10.1002/ca.1086

17. A. T, A. R, A. V, A. F. Effect of supraspinatus deficiency on humerus translation and glenohumeral contact force during abduction. *Clin Biomech*. 2007;22(6):645-651. http://ovidsp.ovid.com/ovidweb.cgi?T=JS&PAGE=reference&D=emed8&NEWS=N&AN=2007262916.

18. Shibata Y. Arthroscopic rotator cuff repair. In: *Advances in Shoulder Surgery*. ; 2016:129-143. doi:10.1007/978-4-431-55988-7_8

19. Shariat A. Rotator cuff repair. In: *Decision-Making in Orthopedic and Regional Anesthesiology: A Case-Based Approach*. ; 2015:163-167. doi:10.1017/CBO9781316145227.031

20. Ozaki J, Fujimoto S, Nakagawa Y, Masuhara K, Tamai S. Tears of the rotator cuff of the shoulder associated with pathological changes in the acromion. A study in cadavera. *J Bone Jt Surg - Ser A*. 1988;70(8):1224-1230. doi:10.2106/00004623-198870080-00015

21. Jerosch J, Müller T, Castro WH. The incidence of rotator cuff rupture. An anatomic study. *Acta Orthop Belg*. 1991;57(2):124-129.

22. Yamaguchi K, Ditsios K, Middleton WD, Hildebolt CF, Galatz LM, Teefey SA. The Demographic and Morphological Features of Rotator Cuff Disease. *J Bone Jt Surg*. 2006;88(8):1699-1704. doi:10.2106/JBJS.E.00835

23. Yamamoto A, Takagishi K, Osawa T, et al. Prevalence and risk factors of a rotator cuff tear in the general population. *J Shoulder Elb Surg*. 2010;19(1):116-120. doi:10.1016/j.jse.2009.04.006

24. Tempelhof S, Rupp S, Seil R. Age-related prevalence of rotator cuff tears in asymptomatic shoulders. *J Shoulder Elb Surg*. 1999;8(4):296-299. doi:10.1016/S1058-2746(99)90148-9

25. Keyes EL. Observations on Rupture of the Supraspinatus Tendon: Based Upon a Study of Seventy-Three Cadavers. *Ann Surg*. 1933;97(6):849-856. https://www.ncbi.nlm.nih.gov/pmc/articles/PMC1391908/pdf/annsurg00627-0050.pdf%0Ahttp://www.ncbi.nlm.nih.gov/pubmed/17866987%0Ahttp://www.pubmedcentral.nih.gov/articlerender.fcgi?artid=PMC1391908.

26. Refior HJ, Krödel A, Melzer C. Examinations of the pathology of the rotator cuff. *Arch Orthop Trauma Surg*. 1987;106(5):301-308. doi:10.1007/BF00454338

27. Needell SD, Zlatkin MB, Sher JS, Murphy BJ, Uribe JW. MR imaging of the rotator cuff: Peritendinous and bone abnormalities in an asymptomatic population. *Am J Roentgenol*. 1996;166(4):863-867. doi:10.2214/ajr.166.4.8610564

28. Crass JR, Craig E V., Feinberg SB. Ultrasonography of rotator cuff tears: A review

of 500 diagnostic studies. *J Clin Ultrasound*. 1988;16(5):313-327. doi:10.1002/jcu.1870160506

29. Goutallier D, Postel J-M, Bernageau J, Lavau L, Voisin M-C. Fatty muscle degeneration in cuff ruptures. Pre- and postoperative evaluation by CT scan. *Clin Orthop Relat Res*. 1994;(304):78-83. doi:10.1097/00003086-199407000-00014

30. Choi S, Kim MK, Kim GM, Roh YH, Hwang IK, Kang H. Factors associated with clinical and structural outcomes after arthroscopic rotator cuff repair with a suture bridge technique in medium, large, and massive tears. *J Shoulder Elb Surg*. 2014;23(11):1675-1681. doi:10.1016/j.jse.2014.02.021

31. Deniz G, Kose O, Tugay A, Guler F, Turan A. Fatty degeneration and atrophy of the rotator cuff muscles after arthroscopic repair: Does it improve, halt or deteriorate? *Arch Orthop Trauma Surg*. 2014;134(7):985-990. doi:10.1007/s00402-014-2009-5

32. Gladstone JN, Bishop JY, Lo IKY, Flatow EL. Fatty infiltration and atrophy of the rotator cuff do not improve after rotator cuff repair and correlate with poor functional outcome. *Am J Sports Med*. 2007;35(5):719-728. doi:10.1177/0363546506297539

33. Klein SM, Dunning P, Mulieri P, Pupello D, Downes K, Frankle MA. Effects of Acquired Glenoid Bone Defects on Surgical Technique and Clinical Outcomes in Reverse Shoulder Arthroplasty. *J Bone Jt Surgery-American Vol*. 2010;92(5):1144-1154. doi:10.2106/JBJS.I.00778

34. Frankle MA, Teramoto A, Luo ZP, Levy JC, Pupello D. Glenoid morphology in reverse shoulder arthroplasty: Classification and surgical implications. *J Shoulder Elb Surg*. 2009;18(6):874-885. doi:10.1016/j.jse.2009.02.013

35. Walch G, Badet R, Boulahia A, Khoury A. Morphologic study of the glenoid in primary glenohumeral osteoarthritis. *J Arthroplasty*. 1999;14(6):756-760. doi:10.3305/nh.2011.26.2.5117

36. Bercik MJ, Kruse K, Yalizis M, Gauci MO, Chaoui J, Walch G. A modification to the Walch classification of the glenoid in primary glenohumeral osteoarthritis using three-dimensional imaging. *J Shoulder Elb Surg*. 2016;25(10):1601-1606. doi:10.1016/j.jse.2016.03.010

37. Sirveaux F, Favard L, Oudet D, Huquet D, Walch G, Molé D. Grammont inverted total shoulder arthroplasty in the treatment of glenohumeral osteoarthritis with massive rupture of the cuff. *J Bone Jt Surg*. 2004;86(3):388-395. doi:10.1302/0301-620X.86B3.14024

38. Lévigne C, Boileau P, Favard L, et al. Scapular notching in reverse shoulder arthroplasty. *J Shoulder Elb Surg*. 2008;17(6):925-935. doi:10.1016/j.jse.2008.02.010

39. Gutiérrez S, Comiskey CA, Luo Z-P, Pupello DR, Frankle MA. Range of Impingement-Free Abduction and Adduction Deficit After Reverse Shoulder Arthroplasty. *J Bone Jt Surgery-American Vol*. 2008. doi:10.2106/jbjs.h.00012

40. Affonso J, Affonso J, Nicholson GP, et al. Complications of the reverse prosthesis: prevention and treatment. *Instr Course Lect*. 2012.

41. Stroud N, DiPaola MJ, Flurin PH, Roche CP. Reverse shoulder glenoid loosening: An evaluation of the initial fixation associated with six different reverse shoulder designs. *Bull NYU Hosp Jt Dis*. 2013;71(SUPPL. 2):12-17.

42. Sutton LG, Werner FW, Jones AK, Close CA, Nanavati VN. Optimization of glenoid fixation in reverse shoulder arthroplasty using 3-dimensional modeling. *J Shoulder Elb Surg*. 2010. doi:10.1016/j.jse.2009.12.003

43. Zumstein MA, Pinedo M, Old J, Boileau P. Problems, complications, reoperations, and revisions in reverse total shoulder arthroplasty: A systematic review. *J Shoulder Elb Surg*. 2011. doi:10.1016/j.jse.2010.08.001

44. Roche CP, Stroud NJ, Martin BL, et al. The impact of scapular notching on reverse

shoulder glenoid fixation. *J Shoulder Elb Surg*. 2013. doi:10.1016/j.jse.2012.10.035

45. Hoenig MP, Loeffler B, Brown S, et al. Reverse glenoid component fixation: is a posterior screw necessary? *J Shoulder Elb Surg*. 2010;19:544-549.

46. Gutiérrez S, Greiwe RM, Frankle MA, Siegal S, Lee WE. Biomechanical comparison of component position and hardware failure in the reverse shoulder prosthesis. *J Shoulder Elb Surg*. 2007;16(3 SUPPL.). doi:10.1016/j.jse.2005.11.008

47. Gutiérrez S, Walker M, Willis M, Pupello DR, Frankle MA. Effects of tilt and glenosphere eccentricity on baseplate/bone interface forces in a computational model, validated by a mechanical model, of reverse shoulder arthroplasty. *J Shoulder Elb Surg*. 2011;20(5):732-739. doi:10.1016/j.jse.2010.10.035

48. Kwon YW, Forman RE, Walker PS, Zuckerman JD. Analysis of reverse total shoulder joint forces and glenoid fixation. *Bull NYU Hosp Jt Dis*. 2010.

49. Chebli C, Huber P, Watling J, Bertelsen A, Bicknell RT, Matsen F. Factors affecting fixation of the glenoid component of a reverse total shoulder prothesis. *J Shoulder Elb Surg*. 2008;17(2):323-327. doi:10.1016/j.jse.2007.07.015

50. Hopkins AR, Hansen UN, Bull AMJ, Emery R, Amis AA. Fixation of the reversed shoulder prosthesis. *J Shoulder Elb Surg*. 2008. doi:10.1016/j.jse.2008.04.012

51. Humphrey CS, Kelly JD, Norris TR. Optimizing glenosphere position and fixation in reverse shoulder arthroplasty, Part Two: The three-column concept. *J Shoulder Elb Surg*. 2008;17(4):595-601. doi:10.1016/j.jse.2008.05.038

52. Parsons BO, Gruson KI, Accousti KJ, Klug RA, Flatow EL. Optimal rotation and screw positioning for initial glenosphere baseplate fixation in reverse shoulder arthroplasty. *J Shoulder Elb Surg*. 2009. doi:10.1016/j.jse.2008.11.002

53. Harman M, Frankle M, Vasey M, Banks S. Initial glenoid component fixation in

"reverse" total shoulder arthroplasty: A biomechanical evaluation. *J Shoulder Elb Surg*. 2005;14(1 SUPPL.):S162-S167. doi:10.1016/j.jse.2004.09.030

54. James J, Huffman KR, Werner FW, Sutton LG, Nanavati VN. Does glenoid baseplate geometry affect its fixation in reverse shoulder arthroplasty? *J Shoulder Elb Surg*. 2012;21(7):917-924. doi:10.1016/j.jse.2011.04.017

55. Stroud NJ, DiPaola MJ, Martin BL, et al. Initial glenoid fixation using two different reverse shoulder designs with an equivalent center of rotation in a low-density and high-density bone substitute. *J Shoulder Elb Surg*. 2013;22(11):1573-1579. doi:10.1016/j.jse.2013.01.037

56. Chebli C, Huber P, Watling J, Bertelsen A, Bicknell RT, Matsen F. Factors affecting fixation of the glenoid component of a reverse total shoulder prosthesis. *J Shoulder Elb Surg*. 2008;17:323-327.

57. Harman M, Frankle M, Vasey M, Banks S. Initial glenoid component fixation in "reverse" total shoulder arthroplasty: a biomechanical evaluation. *J Shoulder Elb Surg*. 2005;14:162S-167S.

58. FRANKLE M, LEVY JC, PUPELLO D, et al. The Reverse Shoulder Prosthesis for Glenohumeral Arthritis Associated with Severe Rotator Cuff Deficiency. *J Bone Jt Surgery-American Vol*. 2006. doi:10.2106/00004623-200609001-00003

59. D. C, D. P, N. V, J. L, M. F. Reverse shoulder arthroplasty for the treatment of rotator cuff deficiency. *J Bone Jt Surg - Ser A*. 2008;90(6):1244-1251. doi:10.2106/JBJS.G.00775 LK - http://vu.on.worldcat.org/atoztitles/link?sid=EMBASE&issn=00219355&id=doi:10.2106%2FJBJS.G.00775&atitle=Reverse+shoulder+arthroplasty+for+the+treatment+of+rotator+cuff+deficiency&stitle=J.+Bone+Jt.+Surg.+Ser.+A&title=Journal+of+Bone+and+Joint+Surgery+-+Series+A&volume=90&issue=6&spage=1244&epage=1251&aulast=Cuff&aufirst=Derek&auinit=D.&aufull=Cuff+D.&coden=JBJSA&isbn=&pages=1244-1251&date=2008&auinit1=D&auinitm=

60. Crosby LA, Hamilton A, Twiss T. Scapula fractures after reverse total shoulder arthroplasty: Classification and treatment. In: *Clinical Orthopaedics and Related Research*. ; 2011. doi:10.1007/s11999-011-1881-3

61. Doornink J, Fitzpatrick DC, Boldhaus S, Madey SM, Bottlang M. Effects of hybrid plating with locked and nonlocked screws on the strength of locked plating constructs in the osteoporotic diaphysis. *J Trauma - Inj Infect Crit Care*. 2010. doi:10.1097/TA.0b013e3181ec9417

62. Estes C, Rhee P, Shrader MW, Csavina K, Jacofsky MC, Jacofsky DJ. Biomechanical strength of the Peri-Loc® proximal tibial plate: A comparison of all-locked versus hybrid locked/nonlocked screw configurations. *J Orthop Trauma*. 2008. doi:10.1097/BOT.0b013e31817279b8

63. Gardner MJ, Griffith MH, Demetrakopoulos D, et al. Hybrid locked plating of osteoporotic fractures of the humerus. *J Bone Jt Surg - Ser A*. 2006. doi:10.2106/JBJS.E.00893

64. Stoffel K, Lorenz KU, Kuster MS. Biomechanical considerations in plate osteosynthesis: The effect of plate-to-bone compression with and without angular screw stability. *J Orthop Trauma*. 2007. doi:10.1097/BOT.0b013e31806dd921

65. Formaini NT, Everding NG, Levy JC, Santoni BG, Nayak AN, Wilson C. Glenoid baseplate fixation using hybrid configurations of locked and unlocked peripheral screws. *J Orthop Traumatol*. 2017. doi:10.1007/s10195-016-0438-3

66. Clark JC, Ritchie J, Song FS, et al. Complication rates, dislocation, pain, and postoperative range of motion after reverse shoulder arthroplasty in patients with and without repair of the subscapularis. *J Shoulder Elb Surg*. 2012. doi:10.1016/j.jse.2011.04.009

67. Hoenig MP, Loeffler B, Brown S, et al. Reverse glenoid component fixation: Is a posterior screw necessary? *J Shoulder Elb Surg*. 2010;19(4):544-549. doi:10.1016/j.jse.2009.10.006

68. Lung TS, Cruickshank D, Grant HJ, Rainbow MJ, Bryant TJ, Bicknell RT. Factors contributing to glenoid baseplate micromotion in reverse shoulder arthroplasty: a biomechanical study. *J Shoulder Elb Surg*. 2019;28(4):648-653. doi:10.1016/J.JSE.2018.09.012

69. Gilot GJ. Addressing glenoid erosion in Reverse Total shoulder arthroplasty. *Bull NYU Hosp Jt Dis*. 2013;71(SUPPL. 2):51-53. doi:10.2307/1928969

70. Gutiérrez S, Comiskey CA, Luo Z-P, Pupello DR, Frankle MA. Range of Impingement-Free Abduction and Adduction Deficit After Reverse Shoulder Arthroplasty. *J Bone Jt Surgery-American Vol*. 2008;90(12):2606-2615. doi:10.2106/JBJS.H.00012

71. Werner CML, Steinmann PA, Gilbart M, Gerber C. Treatment of painful pseudoparesis due to irreparable rotator cuff dysfunction with the Delta III reverse-ball-and-socket total shoulder prosthesis. *J Bone Jt Surg - Ser A*. 2005. doi:10.2106/JBJS.D.02342

72. Cheung E, Willis M, Walker M, Clark R, Frankle MA. Complications in reverse total shoulder arthroplasty. *J Am Acad Orthop Surg*. 2011. doi:10.5435/00124635-201107000-00007

73. Hopkins AR, Hansen UN. Primary stability in reversed-anatomy glenoid components. *Proc Inst Mech Eng H*. 2009;223:805-812.

74. Yang CC, Lu CL, Wu CH, et al. Stress analysis of glenoid component in design of reverse shoulder prosthesis using finite element method. *J Shoulder Elb Surg*. 2013;22(7):932-939. doi:10.1016/j.jse.2012.09.001

75. ASTM. Standard Test Methods for Dynamic Evaluation of Glenoid Loosening or. *Astm*. 2015;i(December):1-7. doi:10.1520/F2028-14.2

76. Westerhoff P, Graichen F, Bender A, et al. In vivo measurement of shoulder joint loads during activities of daily living. *J Biomech*. 2009.

doi:10.1016/j.jbiomech.2009.05.035

77. Collotte P, Erickson J, Vieira TD, Domos P, Walch G. Midterm clinical and radiologic results of reverse shoulder arthroplasty with an eccentric glenosphere. *J Shoulder Elb Surg*. 2020. doi:10.1016/j.jse.2019.09.044

78. Boileau P, Gauci MO, Wagner ER, et al. The reverse shoulder arthroplasty angle: a new measurement of glenoid inclination for reverse shoulder arthroplasty. *J Shoulder Elb Surg*. 2019. doi:10.1016/j.jse.2018.11.074

79. Clavert P, Kling A, Sirveaux F, et al. Reverse shoulder arthroplasty for instability arthropathy. *Int Orthop*. 2019. doi:10.1007/s00264-018-4123-4

80. Boileau P, Morin-Salvo N, Gauci MO, et al. Angled BIO-RSA (bony-increased offset–reverse shoulder arthroplasty): a solution for the management of glenoid bone loss and erosion. *J Shoulder Elb Surg*. 2017. doi:10.1016/j.jse.2017.05.024

81. Königshausen M, Sverdlova N, Ehlert C, et al. Bone grafting in oblique versus prepared rectangular uncontained glenoid defects in reversed shoulder arthroplasty. A biomechanical comparison. *Clin Biomech*. 2017;50(September):7-15. doi:10.1016/j.clinbiomech.2017.09.011

82. Roche CP, Stroud NJ, Martin BL, et al. Achieving fixation in glenoids with superior wear using reverse shoulder arthroplasty. *J Shoulder Elb Surg*. 2013;22(12):1695-1701. doi:10.1016/j.jse.2013.03.008

83. Klein SM, Dunning P, Mulieri P, Pupello D, Downes K, Frankle MA. Effects of acquired glenoid bone defects on surgical technique and clinical outcomes in reverse shoulder arthroplasty. *J Bone Jt Surg - Ser A*. 2010;92(5):1144-1154. doi:10.2106/JBJS.I.00778

84. Bryce CD, Pennypacker JL, Kulkarni N, et al. Validation of three-dimensional models of in situ scapulae. *J Shoulder Elb Surg*. 2008;17(5):825-832. doi:10.1016/j.jse.2008.01.141

85. Knowles NK, Keener JD, Ferreira LM, Athwal GS. Quantification of the position, orientation, and surface area of bone loss in type B2 glenoids. *J Shoulder Elb Surg*. 2015;24(4):503-510. doi:10.1016/j.jse.2014.08.021

86. Knowles NK, Keener JD, Ferreira LM, Athwal GS. Quantification of the position, orientation, and surface area of bone loss in type B2 glenoids. *J Shoulder Elb Surg*. 2015;24(4):503-510. doi:10.1016/j.jse.2014.08.021

87. Somerson JS, Hsu JE, Gorbaty JD, Gee AO. Classifications in Brief: Goutallier Classification of Fatty Infiltration of the Rotator Cuff Musculature. *Clin Orthop Relat Res*. 2016;474(5):1328-1332. doi:10.1007/s11999-015-4630-1

88. Fuchs B, Weishaupt D, Zanetti M, Hodler J, Gerber C. Fatty degeneration of the muscles of the rotator cuff: Assessment by computed tomography versus magnetic resonance imaging. *J Shoulder Elb Surg*. 1999;8(6):599-605. doi:10.1016/S1058-2746(99)90097-6

89. Müller CT, Buck FM, Mamisch-Saupe N, Gerber C. Good correlation of goutallier rating of supraspinatus fatty changes on axial and reformatted parasagittal computed tomographic images. *J Comput Assist Tomogr*. 2014;38(3):340-343. doi:10.1097/RCT.0000000000000059

90. Trudel G, Ryan SE, Rakhra K, Uhthoff HK. Extra- and Intramuscular Fat Accumulation Early after Rabbit Supraspinatus Tendon Division: Depiction with CT. *Radiology*. 2010;255(2):434-441. doi:10.1148/radiol.10091377

91. Boileau P, Moineau G, Roussanne Y, O'Shea K. Bony increased-offset reversed shoulder arthroplasty minimizing scapular impingement while maximizing glenoid fixation. In: *Clinical Orthopaedics and Related Research*. Vol 469. ; 2011:2558-2567. doi:10.1007/s11999-011-1775-4

92. Levy JC, Virani N, Pupello D, Frankle M. Use of the reverse shoulder prosthesis for the treatment of failed hemiarthroplasty in patients with glenohumeral arthritis and rotator cuff deficiency. *J Bone Jt Surg - Br Vol*. 2007;89-B(2):189-195.

doi:10.1302/0301-620X.89B2.18161

93. Hoenig MP, Loeffler B, Brown S, et al. Glenoid Baseplate Micromotion in Reverse Total Shoulder Arthroplasty. *J Shoulder Elb Surg*. 2008;17(11):1-7. doi:10.1016/j.jbiomech.2004.01.031

94. Neyton L, Boileau P, Nové-Josserand L, Edwards TB, Walch G. Glenoid bone grafting with a reverse design prosthesis. *J Shoulder Elb Surg*. 2007;16(3 SUPPL.):71-78. doi:10.1016/j.jse.2006.02.002

95. Norris TR, Kelly JD, Humphrey CS. Management of glenoid bone defects in revision shoulder arthroplasty: A new application of the reverse total shoulder prosthesis. *Tech Shoulder Elb Surg*. 2007;8(1):37-46. doi:10.1097/BTE.0b013e318030d3b7

96. K.E. W, X.C. S, B.J. J, J.P. I, E.T. R. Progression of glenoid morphology in glenohumeral osteoarthritis. *J Bone Jt Surg - Am Vol*. 2018;100(1):49-56. doi:10.2106/JBJS.17.00064 LK - http://vu.on.worldcat.org/atoztitles/link?sid=EMBASE&issn=15351386&id=doi:10.2106%2FJBJS.17.00064&atitle=Progression+of+glenoid+morphology+in+glenohumeral+osteoarthritis&stitle=J.+Bone+Jt.+Surg.+Am.+Vol.&title=Journal+of+Bone+and+Joint+Surgery+-+American+Volume&volume=100&issue=1&spage=49&epage=56&aulast=Walker&aufirst=Kyle+E.&auinit=K.E.&aufull=Walker+K.E.&coden=JBJSA&isbn=&pages=49-56&date=2018&auinit1=K&auinitm=E

97. Martin EJ, Duquin TR, Ehrensberger MT. Reverse total shoulder glenoid baseplate stability with superior glenoid bone loss. *J Shoulder Elb Surg*. 2017;26(10). doi:10.1016/j.jse.2017.04.020

98. Knowles NK, Ferreira LM, Athwal GS. Augmented glenoid component designs for type B2 erosions: A computational comparison by volume of bone removal and quality of remaining bone. *J Shoulder Elb Surg*. 2015;24(8):1218-1226. doi:10.1016/j.jse.2014.12.018

99. Allred JJ, Flores-Hernandez C, Hoenecke HR, D'Lima DD. Posterior augmented glenoid implants require less bone removal and generate lower stresses: A finite element analysis. *J Shoulder Elb Surg*. 2016. doi:10.1016/j.jse.2015.10.003

100. Kersten AD, Flores-Hernandez C, Hoenecke HR, D'Lima DD. Posterior augmented glenoid designs preserve more bone in biconcave glenoids. *J Shoulder Elb Surg*. 2015;24(7):1135-1141. doi:10.1016/j.jse.2014.12.007

101. Donohue KW, Ricchetti ET, Ho JC, Iannotti JP. In fi ltration and Glenoid Morphology in. 2018:381-387.

102. Mahaffy MD, Knowles NK, Berkmortel C, et al. Density distribution of the type E2 glenoid in cuff tear arthropathy. *J Shoulder Elb Surg*. 2020. doi:10.1016/j.jse.2019.05.046

Curriculum Vitae

Name:	Šejla (Sheyla) Abdić
Post-secondary Education and Degrees:	The University of Western Ontario London, Ontario, Canada 2019-2020 M.Sc. Surgery Paracelsus Medical University Salzburg, Austria 2014-2019 M.D. York University North York, Ontario, Canada 2005-2012 B.Sc. Honors
Honours and Awards:	Hospital for Special Surgery/Weill Cornell Medical University: Max-Kade Clinical Clerkship Scholarship (1,000 USD) 2019 Paracelsus Medical University Scientific Congress Speaker Award. (450 EUR) 2019 Paracelsus Medical University Diploma Thesis Travel Award. (1,000 EUR) 2018 Paracelsus Medical University Annual Academic Award. 9,000 EUR annually (45,000 EUR) 2014-2019 “Start Something with Alesse” by Pfizer business grant for (5,000 CAD) 2011-2012 Millennium Excellence Grant (2,500 CAD) 2009 Millennium Excellence Award (10,000 CAD) 2007-2008

Related Work Experience:	Medical Device Innovation Fellow The University of Western Ontario WorlDiscoveries, BrainsCAN 2020-2021

Publications:

1. **Abdic S**, Lockhart J, Alnusif N, Johnson JA, Athwal GA. *Glenoid Baseplate Screw Fixation in Reverse Shoulder Arthroplasty: Does Locking Screw Position and Orientation Matter?* J Shoulder Elbow Surg. (accepted Jul 2020)
2. **Abdic S**, Knowles NK, Johnson JA, Walch G, Athwal GS. *Type E2 Glenoid Bone Loss Orientation and Management with Augmented Implants*. J Shoulder Elbow Surg. (Nov 2019)
3. Mahaffy MD, Knowles NK, Berkmortel C, **Abdic S**, Walch G, Johnson JA, Athwal GS. *Density Distribution of the Type E2 Glenoid in Cuff Tear Arthropathy*. J Shoulder Elbow Surg. (Aug 2019)
4. **Abdic S,** Athwal GS, Walch G, Raiss P. *Short Stem Humeral Components in Reverse Shoulder Arthroplasty: Stem Alignment Influences the Neck Shaft Angle*. Arch Orthop Traum Su. (March 2020)
5. Moroder P, Plachel F, Becker J, Schulz E, **Abdic S**, Haas M, Resch H. *Clinical and Radiological Long-Term Results after Implant-Free Autologous Pelvic Bone Graft Procedure (J-Span) for the Treatment of Anterior Shoulder Instability*. Am J Sports Med. (Oct 2018)
6. Plachel F, Korn G, **Abdic S**, Moroder P. *Acute Locked Superior Shoulder Dislocation in a Patient with Cuff Tear Arthropathy*. BMJ Case Reports (June 2018)
7. Moroder P, Plachel F, **Abdic S**, Resch H. *Shoulder and Elbow Injuries in Athletes: Prevention, Treatment and Return to Sport. Textbook chapter "Subscapularis: Pectoralis Major Transfer"*. Elsevier, 2017.
8. **Abdic S.** Author and editor of *"Making It In High Heels 3: Innovators and Trailblazers"*, a motivational book for women about success. Burman Books, 2013.